1

DENDRIMERS AS QUANTIZED NANO-MODULES IN THE NANOTECHNOLOGY FIELD

JØRN B. CHRISTENSEN[1] AND DONALD A. TOMALIA[2,3]

[1]*Department of Chemistry, University of Copenhagen, DK-2100 Copenhagen, Denmark*

[2]*The National Dendrimer & Nanotechnology Center, Department of Chemistry, Central Michigan University, Mt. Pleasant, MI, 48859 USA*

[3]*NanoSynthons LLC, 1200 N. Fancher Ave., Mt. Pleasant, MI, 48858 USA*

1.1 INTRODUCTION

According to an insightful opinion expressed by Nobel Laureate, R. Hoffmann [1], chemistry and physics meet in the solid state where these two disciplines share a significant mutual interest concerning the structure of matter. That withstanding, chemists are usually most concerned with the use of atom building blocks and the manipulation of their electrons to produce more complex molecular structure. Historically, much of this earlier activity focused on the evolution of first principles and a "central paradigm" as briefly outlined in Figure 1.1.

These first principles led to the emergence of "elemental periodicity" that ultimately produced Mendeleev's Periodic Table (1869), and a systematic framework for unifying and defining the very rich contemporary science of traditional small molecule and macromolecular chemistry. One of the greatest challenges facing today's interdisciplinary field of nanoscience is the absence of a "central paradigm," and a nanomaterials classification roadmap for organizing and defining the growing number of nanostructures and assemblies that are being reported in the literature. These issues were examined as a critical theme for a recent National Science
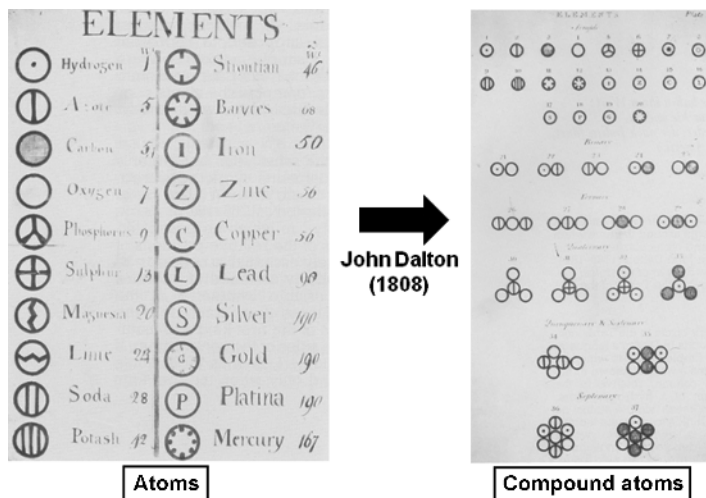
- Atoms form chemical bonds
- Atoms bond with discrete stoichimetries, valency, and combining weights
- Atoms bond with discrete directionality
- Atoms exhibit periodic properties

FIGURE 1.1   Dalton's first table of elemental atoms and their conversion to compound atoms according to his atom/molecular hypotheses. Key components of traditional chemistry central dogma based on Dalton's hypothesis [2].

Foundation (NSF) workshop entitled: "Periodic Patterns, Relationships and Categories of Well-Defined Nanoscale Building Blocks" [3]. An embryonic consensus of principles, classifications, and fundamentals emerged from this workshop that has now evolved into a systematic framework for unifying and defining nanoscience. This conceptual framework was based on historical principles, which were first used for traditional chemistry and included: (a) a nanomaterials classification roadmap, (b) a table of well-defined nano-module (element) categories, (c) combinatorial libraries of nano-compounds/-assemblies, and (d) the observation of nano-periodic property patterns. This concept was recently published [4]. It focused exclusively on well-defined monodisperse (0-D/1-D) nanoscale materials and the division of these well-defined materials into hard and soft nanoparticles (i.e., modules) following elemental compositional and architectural criteria invoked for traditional inorganic and organic materials (Figure 1.2). These well-defined nano-modules were selected based on criteria associated with traditional features/behavior of atoms (i.e., atom mimicry) and were referred to as hard and soft particle nano-element categories. As such, these nano-element categories mimic atoms by reacting or self-assembling to form combinatorial libraries of hard–hard, hard–soft, or soft–soft nano-compounds or nano-assemblies. Finally, due to the conserved nature of the precursor building blocks (i.e., atoms and/or small molecules) leading to these well-defined nano-element categories and their nano-compounds/-assemblies, many nano-periodic property
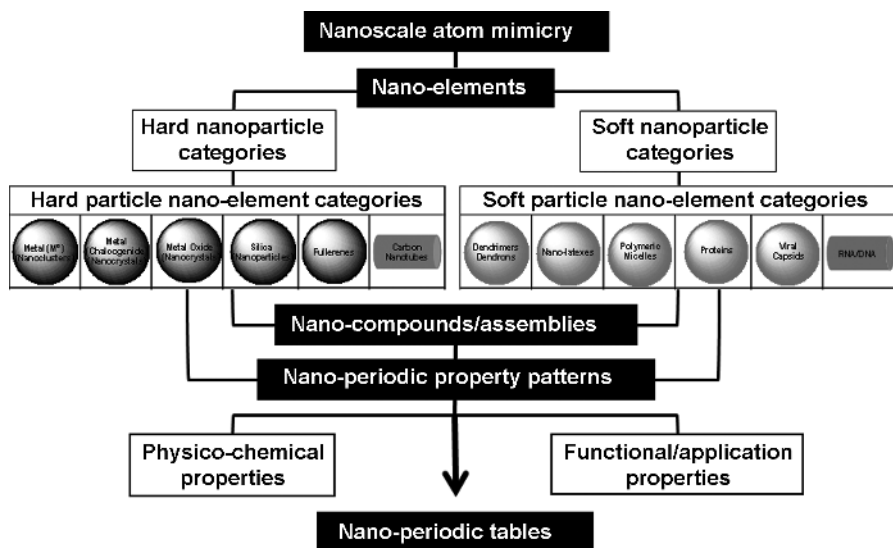
FIGURE 1.2 Concept overview. Using first principles and step logic that led to the "central dogma" for traditional chemistry, the criteria of nanoscale atom mimicry was applied to Category I-type, well-defined nanoparticles. This produced 12 proposed nano-element categories, which were classified into six hard particle and six soft particle nano-element categories. Chemically bonding or assembling these hard and soft nano-elements leads to hard:hard, soft: hard, or soft:soft type nano-compound categories, many of which have been reported in the literature. Based on the discrete, quantized features associated with the proposed nano-elements and their compounds, an abundance of nano-periodic property patterns related to their intrinsic physicochemical and functional/application properties have been observed and reported in the literature.

patterns have been observed and reported in the literature. These nano-property trends/periodic property patterns may be classified as either intrinsic physicochemical or functional/application type properties. In all cases these unique nano-property trends/patterns appear to be inextricably related to well controlled *c*ritical *n*anoscale *d*esign *p*arameters (CNDPs), such as size, shape, surface chemistry, flexibility, and architecture as overviewed in Figure 1.2.

This account will focus only on dendrons/dendrimers that have been previously reported to exhibit many features associated with traditional elemental atoms (i.e., *atom mimicry*) [5,6]. Inspired by these early examples of dendrimer-based heuristic atom mimicry, a broader concept was evolved which embraced both hard and soft particle nano-element categories. Presently, six hard nano-element and six soft nano-element categories have been proposed. Dendrons/dendrimers constitute one of the six proposed *soft particle, nano-element categories, namely the [S-1]; core–shell type category in this* nano-periodic system. As such, dendrimers behave as *soft particle nano-elements* to produce well-characterized core–shell (tecto) dendrimers (i.e., *dendrimer–dendrimer type nano-compounds*). Similarly, reactions with fullerenes have been reported to produce stoichiometric *dendrimer–fullerene*

type nano-compounds [7], whereas, dendrimers bearing either surface or interior ligation sites reacted with metal salts to produce stoichiometric *dendrimer–metal ligation type nano-compounds* [8,9]. Some of these constructs could be further reduced to yield *core–shell; dendrimer–metal nano-cluster type nano-compounds*. These results optimistically portend the extension of this concept to a wide variety of other well-defined soft particle nano-element categories (i.e., proteins, DNA/RNA, viral capsids, etc.), and hard particle nano-element categories (i.e., metal oxide nanocrystals, metal chalcogenide nanocrystals, fullerenes, etc.).

1.2   CRITICAL NANOSCALE DESIGN PARAMETERS (CNDPs): STRUCTURAL CONTROL IN DENDRIMERS

Dendrimers are widely recognized as an important subclass within the fourth major polymer architecture category referred to as (IV) *dendritic polymers* [10] (see Figure 1.3). Hierarchically speaking, dendrimers are collections of 10^3–10^4 atoms with relative molar masses of 10^4–10^5 Da and hydrodynamic dimensions ranging from 1 to 30 nm. Among the most important features of dendrimers is that they can be synthesized with precise structural control over their CNDP's, which include nanoscale: (a) *sizes*, (b) *shapes*, (c) *surface chemistries*, (d) *flexibilities/ rigidities*, and (e) *architecture* [11]. This is in sharp contrast to statistical poly-dispersed features which are normally associated with traditional polymer archi-tectures, namely: (I) linear, (II) cross-linked polymers, and (III) branched types as shown in Figure 1.3.
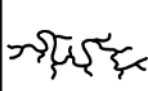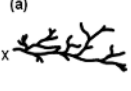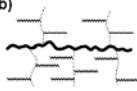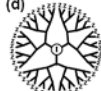

FIGURE 1.3   Four major classes of macromolecular architecture. Traditional synthetic polymers: (I) linear, (II) cross-linked (bridged), and (III) branched. Structure controlled polymers (IV) dendritic.

1.2.1 Dendrimer Synthesis: Divergent and Convergent Methods

In contrast to traditional polymers, dendrimers are monodisperse, macromolecular core–shell structures, consisting of three basic architectural components, namely: (1) a core, (2) an interior of monomer shells (generations) consisting of repeating branch-cell units, and (3) terminal functional groups (i.e., the outer shell or periphery). Dendrimer synthesis strategies may be divided into two major approaches and are referred to as either a *divergent* or *convergent* assembly strategies. The required building blocks and synthetic pathways are as outlined in Figure 1.4.
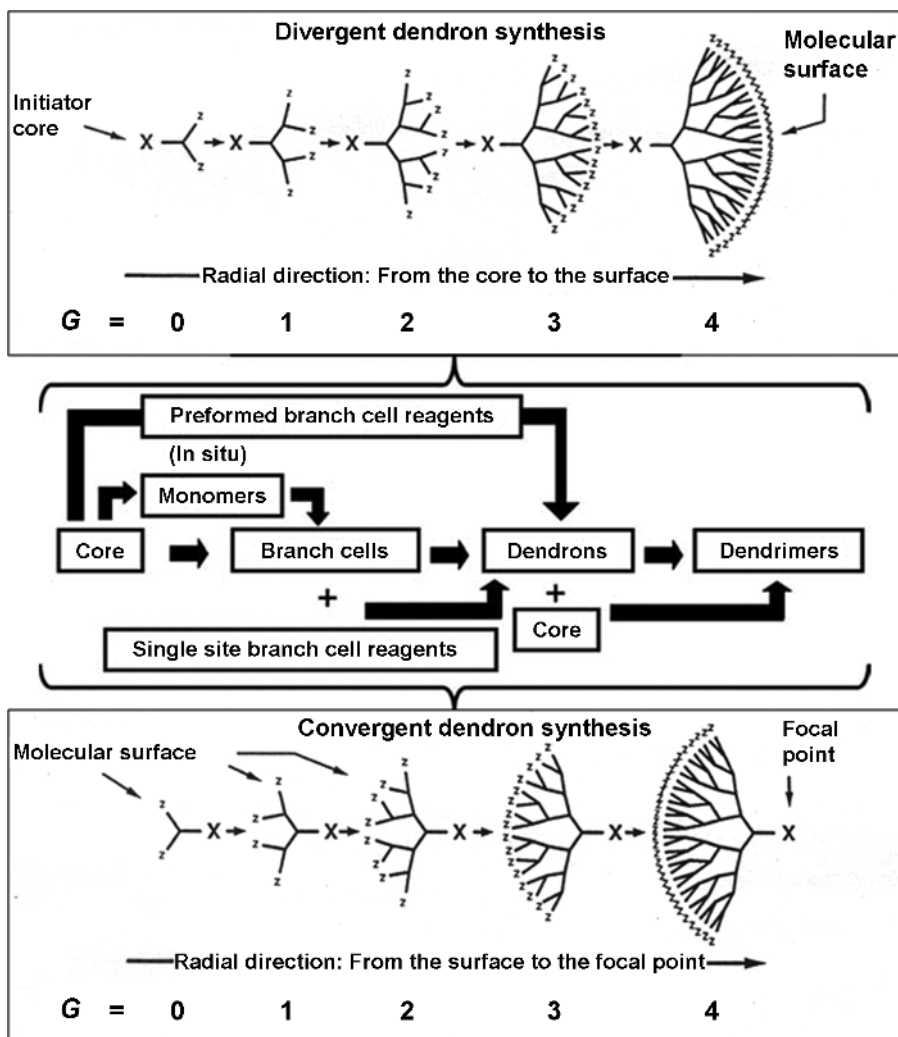

FIGURE 1.4 Hierarchical assembly scheme illustrating the options for constructing dendrimers by either divergent (Tomalia-type) or convergent (Frechet-type) synthetic strategies.

In general, dendrimers produced by the convergent strategy are nearly free of defects. This is in contrast to dendrimers obtained by the divergent approach; wherein, low defect levels are observed in the early generations with substantially higher defect levels occurring at higher generations (Figure 1.4). A comparison is made between *convergent*—Yamamoto-type dendrimers and *divergent*—Meijer-type dendrimers as shown in Figures 1.6 and 1.7, respectively.

Within each of these major approaches, there may be variations in methodology for branch-cell or dendron construction, (i.e., supramolecular assembly [12], click chemistry [13], etc.). Many of these issues, together with experimental laboratory procedures, have been extensively reviewed elsewhere [14–19].

1.2.2 Quantized Component Relationships to Produce Core–Shell, Soft Nano-Matter Dendrimer Structures

The steps required for the divergent assembly of dendrimers may be thought of as beginning with quantized, core information. This core information that defines initiator size, shape, multiplicity, and directionality then orchestrates subsequent iterative monomer shell polymerization events. The resulting monomer shells (i.e., generations) consist of mathematically defined numbers of monomers and branch-cell domains, which are required to produce these discrete nanoscale core–shell structures. As such, dendrimers may be viewed as nanoscale processing devices; wherein, their precise sizes and shapes are directed and controlled as illustrated in Figure 1.5.

Each architectural component manifests a specific function, and at the same time defines important periodic properties for these nanostructures as they are grown generation by generation. For example, as illustrated in Figure 1.5 the *core* may be thought of as the molecular information center from which *size*, *shape*, *directionality, and multiplicity* are expressed *via* covalent connectivity to the outer shells [11]. Within the *interior*, one finds the *branch-cell amplification region*, which defines the type and amount of interior void space that may be enclosed by the terminal groups as the dendrimer is grown to a surface congested level (Figure 1.9).

Branch-cell multiplicity (N_b) determines the density and degree of amplification as an exponential function of generation (G) (Figure 1.8). The interior composition and amount of solvent-filled void space determines the extent and nature of guest–host (endo-receptor) properties (i.e., for encapsulation of metals, pharma, or small guest molecules) that is possible with a particular dendrimer family and generation (Figure 1.24). Finally, the surface may consist of either reactive or passive terminal groups that may perform a variety of functions. With appropriate function, they serve as a *template polymerization region*; wherein, each generation is amplified and covalently attached to the precursor generation.

Secondly, the surface groups may function as passive or reactive gates controlling entry or departure of guest molecules from the dendrimer interior. These three architectural components essentially determine a rich range of nano-physicochemical properties, and the overall sizes, shapes, reactivity, and flexibility of dendrimers. It is important to note that dendrimer diameters increase linearly as a function of shells or
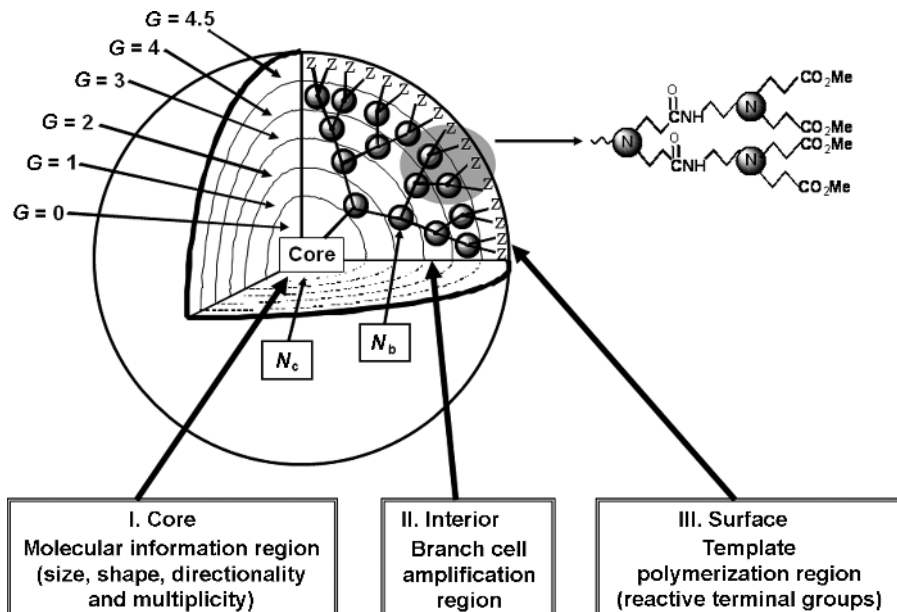
FIGURE 1.5 Tomalia type ($G = 4.5$); {*dendri*-poly(amidoamine)-(CO$_2$Me)$_Z$}; (PAMAM) dendrimers. A 3-D projection of such a dendrimer core–shell architecture for $G = 4.5$ poly (amidoamine) (PAMAM) dendrimer with principal architectural components (I) core, (II) interior, and (III) surface [20].

generations added; whereas, the terminal functional groups increase exponentially (Figure 1.8) as a function of generation. This dilemma enhances "tethered congestion" of the anchored dendrons, as a function of generation, due to the steric crowding of the end groups. As a consequence, lower generations are generally open, floppy structures; whereas, higher generations become robust, less deformable spheroids, ellipsoids, or cylinders [23] depending on the shape and multiplicity of the core.

1.3 EXPERIMENTALLY PROVEN STRUCTURAL CONTROL OF CRITICAL NANOSCALE DESIGN PARAMETERS (CNDPs)

In this section, we focus on experimentally proven examples that illustrate structural control of CNDP's when synthesizing dendrons/dendrimers. This brief overview illustrates examples of atom mimicry based on the synthetic ability to control; (a) *sizes*, (b) *shapes*, (c) *surface chemistry*, (d) *flexibility*, and (e) *architecture at the nanoscale level*. It is apparent, that both the core multiplicity (N_c) and branch-cell multiplicity (N_b) determine the precise number of terminal groups (Z) and mass amplification as a function of generation (G). One may view those generation sequences as quantized polymerization events that adhere to the dendritic aufbau
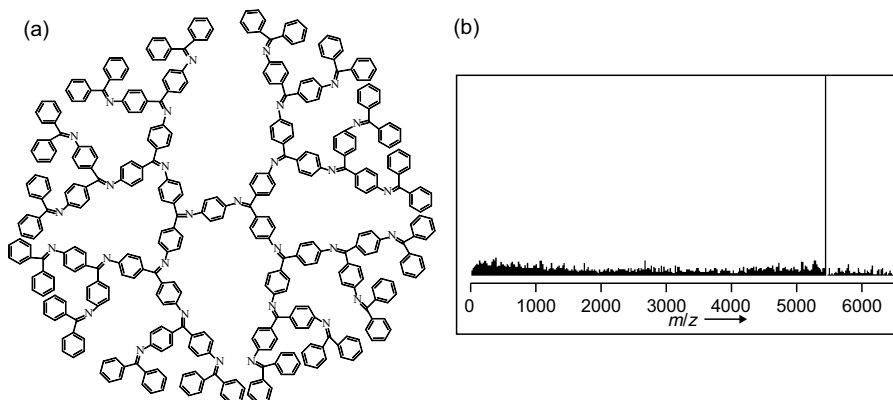
FIGURE 1.6 (a) Yamamoto-type [core:*p*-phenylene]; ($G = 4$); {*dendri*-poly(phenylazomethine)} (DPA) dendrimers, (b) MALDI-TOF of the G4; DPA dendrimer [21]. Copyright 2001 American Chemical Society.

mathematics described in Figure 1.9. The assembly of reactive monomers [11,24], branch cells [11,25,26], or dendrons [12,27] around atomic or molecular cores to produce dendrimers according to divergent/convergent dendritic branching principles has been well demonstrated (Figure 1.4). This systematic filling of nano-space around cores with branch cells in generational growth stages (branch-cell shells) produces discrete, quantized bundles of mass that are mathematically predictable [5]. Predicted molecular weights are routinely confirmed by mass spectroscopy [22,28,29] (Figures 1.6 and 1.7) and other analytical methods [27,30–32]. Predicted numbers of branch cells, terminal groups (Z), and molecular weights, as a function of generation, are as described in Figure 1.8. It should be noted, that the molecular weights approximately double as one progresses from one generation to the next. The surface groups (Z) and branch cells (BC) amplify mathematically according to a power function; thus, producing discrete, monodisperse structures with precise molecular weights. These predicted values are routinely verified for convergent synthesized dendrimers by mass spectroscopy (Figure 1.6). However, for divergent synthesized dendrimers, minor mass defects are often observed for higher generations as congestion induced *de Gennes dense packing* and nano-steric effects begin to occur [11,33] (Figure 1.7).

1.3.1 Quantized Size-Control of Monodisperity

The bottom-up synthesis of dendrons/dendrimers provides one of the most precise and tunable strategies known for constructing a systematic continuum of reproducible soft matter nanoscale structures. Size and structure control observed for dendron/dendrimer synthesis rival that expected for proteins and DNA/RNA. In fact, dendrimers are often referred to as *artificial proteins* [34–36]. Based on the close mimicry of globular protein size scaling and their monodispersity, they are often used as protein replacements/substitutes in many nanomedicinal applications [34,35,37,38].
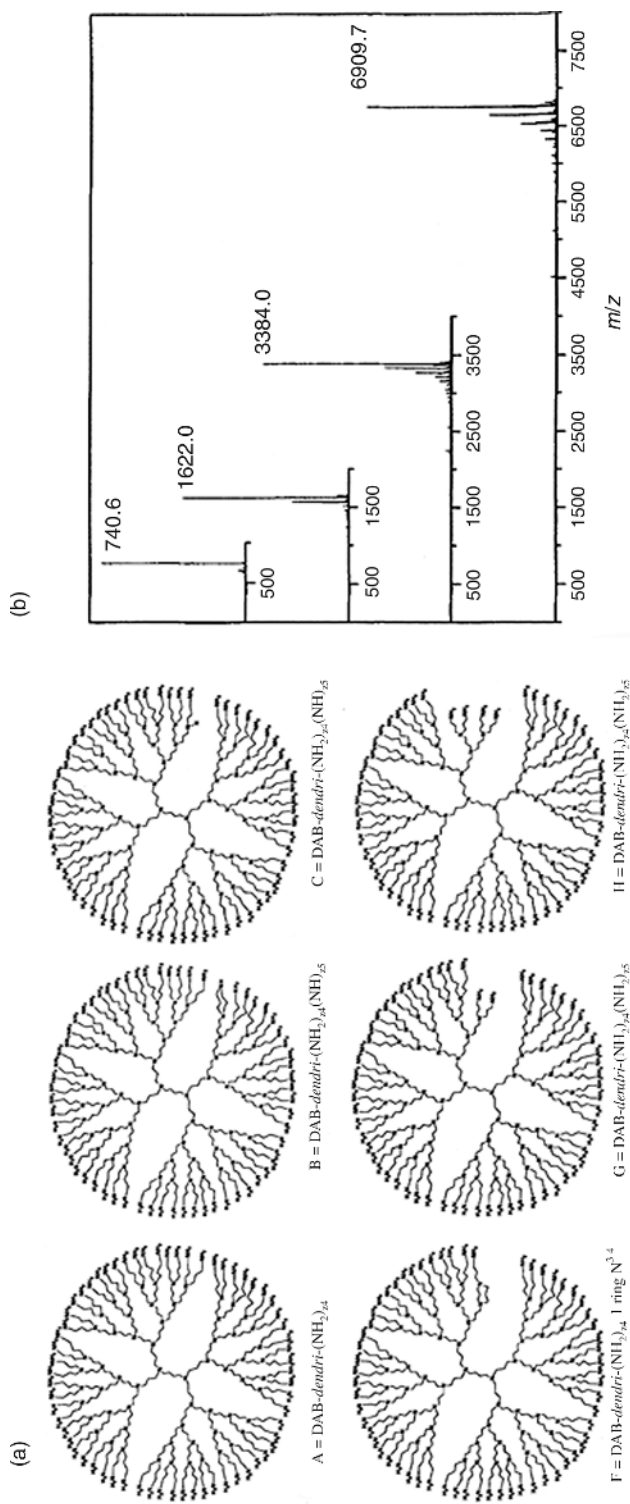
FIGURE 1.7 (a) Meijer-type [core:diaminobutane]; $(G = 4)$; {*dendri*-poly(propyleneimine)-$(NH_2)_Z$} (PPI) dendrimers illustrating perfect structure and defective structures observed by mass spectrometry; (b) deconvoluted ESI-MS data showing masses for perfect structures and defective structures for PPI dendrimers; $G = 1–4$ [22]. Copyright Wiley-VCH Verlag Gmbh & Co. KGaA.
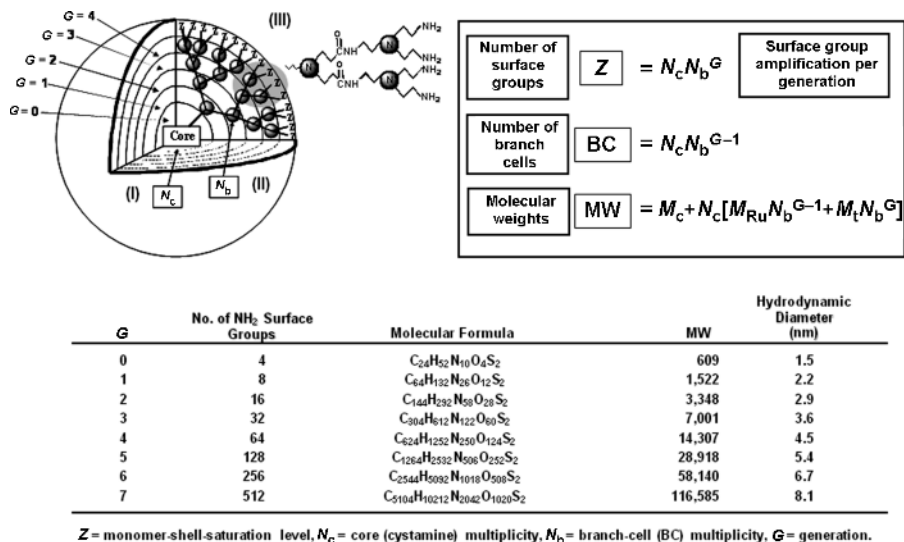
9

Number of surface groups	Z	$= N_c N_b{}^G$	Surface group amplification per generation
Number of branch cells	BC	$= N_c N_b{}^{G-1}$	
Molecular weights	MW	$= M_c + N_c[M_{Ru} N_b{}^{G-1} + M_t N_b{}^G]$	

G	No. of NH_2 Surface Groups	Molecular Formula	MW	Hydrodynamic Diameter (nm)
0	4	$C_{24}H_{52}N_{10}O_4S_2$	609	1.5
1	8	$C_{64}H_{132}N_{26}O_{12}S_2$	1,522	2.2
2	16	$C_{144}H_{292}N_{58}O_{28}S_2$	3,348	2.9
3	32	$C_{304}H_{612}N_{122}O_{60}S_2$	7,001	3.6
4	64	$C_{624}H_{1252}N_{250}O_{124}S_2$	14,307	4.5
5	128	$C_{1264}H_{2532}N_{506}O_{252}S_2$	28,918	5.4
6	256	$C_{2544}H_{5092}N_{1018}O_{508}S_2$	58,140	6.7
7	512	$C_{5104}H_{10212}N_{2042}O_{1020}S_2$	116,585	8.1

Z = monomer-shell-saturation level, N_c = core (cystamine) multiplicity, N_b = branch-cell (BC) multiplicity, G = generation.

FIGURE 1.8 Mathematical expressions for calculating the theoretical number of surface groups (Z), branch cells (BC), and molecular weights (Mw) for [*core*:1, cystamine]; ($G = 0$–7); {*dendri*-poly(amidoamine)-$(NH_2)_Z$} (PAMAM) dendrimers as a function of generation. Approximate hydrodynamic diameters ($G = 0$–7) based on gel electrophoretic comparison for the corresponding PAMAM dendrimers.

Dendrimer mass and size uniformity has been exhaustively demonstrated by ESI/MALDI-TOF mass spectrometry [29], gel electrophoresis [30–32,39], electron microscopy (TEM) [40], (Figure 1.10), atomic force microscopy (AFM) [41] and other methodologies, to mention a few [42]. Within a specific dendrimer family, it is possible to produce a systematic, reproducible continuum of nano-sizes and precise masses as a function of generations (see Figures 1.8–1.10). It should be noted, that dendrimer mass approximately doubles, generation to generation, with a remarkable uniformity of mass distribution over five generations exhibiting polydispersities ranging from 1.005 to 1.130.

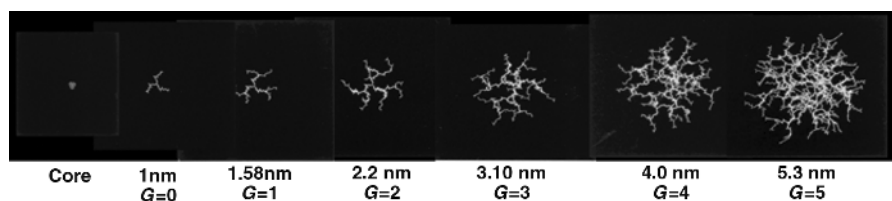| Core | 1nm G=0 | 1.58nm G=1 | 2.2 nm G=2 | 3.10 nm G=3 | 4.0 nm G=4 | 5.3 nm G=5 |

FIGURE 1.9 Molecular simulations for [core:NH_3]; ($G = 0$–5); {*dendri*-poly(amidoamine)-$(NH_2)_n$} (PAMAM) dendrimers and a generational comparison of hydrodynamic diameters. (See the color version of this figure in Color Plates section.)

1.3.2   Quantized Shapes of Dendrimers

Several simple parameters may be used to design and control covalent dendrimer shape. As described in Figures 1.5 and 1.11, the multiplicity and the shape of the core can be selected to produce a desired shape (i.e., spheroidal, ellipsoidal, cylindrical, etc.). For example, covalent 1-D cylindrical dendrimers are readily synthesized with shape control by dendronization or initiating dendron growth from multiple sites along the backbone of a linear polymer [23,43]. Iterative monomer additions to produce generational growth will then produce precise amplifications of these programmed shapes. The rigidity/flexibility of these shapes may be controlled and tuned by appropriate selection of branch-cell monomer symmetry, compositions, and arm lengths (flexibility).

Pioneering work by Rudick and Percec [44], demonstrated that quantized shape design of dendrons as a function of their generation level produced predictable hierarchical patterns of periodic nano-object shapes that could be defined as solid angle projections (α') of the dendron onto a plane (Figure 1.11). The (α') angle is defined as the projection of the solid angle of the dendron onto a plane, and can be
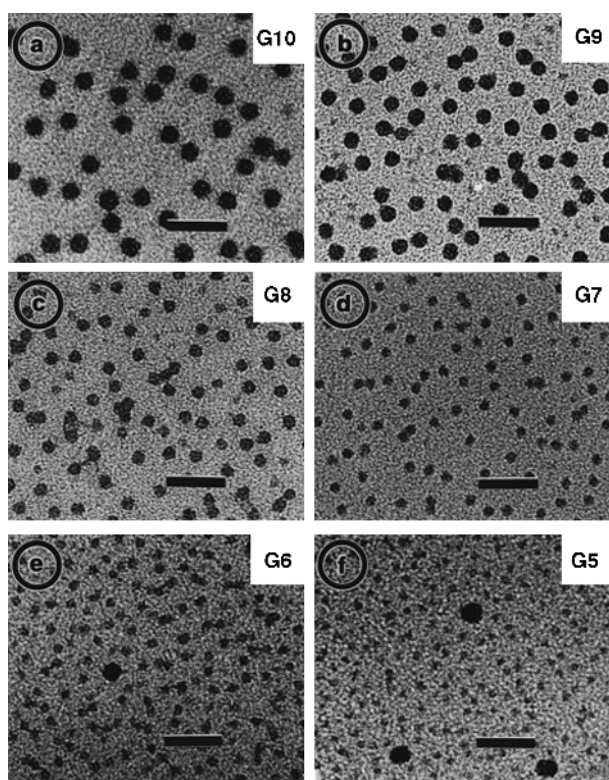

FIGURE 1.10   (a–f) Transmission electron micrographs (TEMs) of $G = 5$–10 PAMAM dendrimers. Sample (f) contains three molecules of $G = 10$ dendrimer for comparison. Bar length $= 50$ nm [40]. Copyright 1998 American Chemical Society.
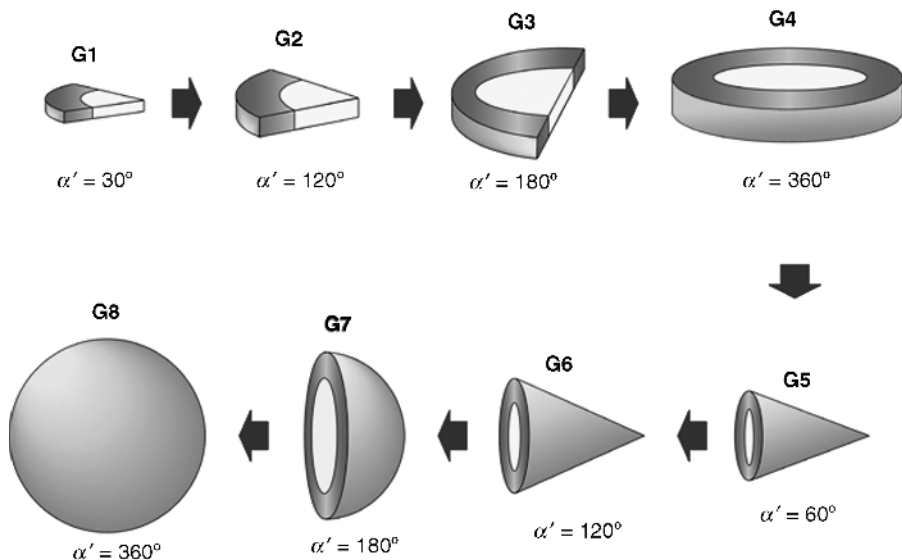
FIGURE 1.11   Hierarchical control of self-assembly *via* molecular solid angle [46].

determined in all cases according to $(\alpha') = 360/u$, where u is the number of dendrons in a column stratum or supramolecular sphere. Increasing the branching *via* a change in sequence or increase in generation number of taper-like dendrons increases the (α') and the fraction of the disk occupied in columnar self-assembly. At a certain threshold only unimolecular disks are formed. Above this threshold, further branching results in deformation of the disk into a conical segment with diminished (α'). Beyond this point, increased branching increases (α') and the fraction of a sphere formed. Ultimately, a unimolecular sphere should result. A wide variety of periodic and quasiperiodic lattices can be formed by simply tuning the dendron shape parameters as described in Figure 1.12 [45].

1.3.3   Quantized Surface Chemistry

More than 1000 different surface reactions have been reported for dendrons/ dendrimers. Essentially, all mechanistic reaction types (i.e., covalent, ionic, radical, etc.) have been reported. Several examples of these reactions are illustrated in Figure 1.13. Both subnanoscale, and nanoscale reagents (i.e., proposed nano-elements) have been used in these surface reactions. The surface valency and stoichiometry are mathematically quantified by relationships described in Figure 1.8 (i.e., $Z = N_c N_b{}^G$). Generally, these valencies and stoichiometric binding ratios are operational for all generations preceding serious onset of de Gennes-type dense packing congestion. Surface congested generations (i.e., $>G = 4$ for poly(amidoamine) (PAMAM) dendrimers) usually exhibit lower than theoretical stoichiometries even with small-sized reagents. Large-sized reagents (i.e., >1 nm) may lead to less than ideal stoichiometries
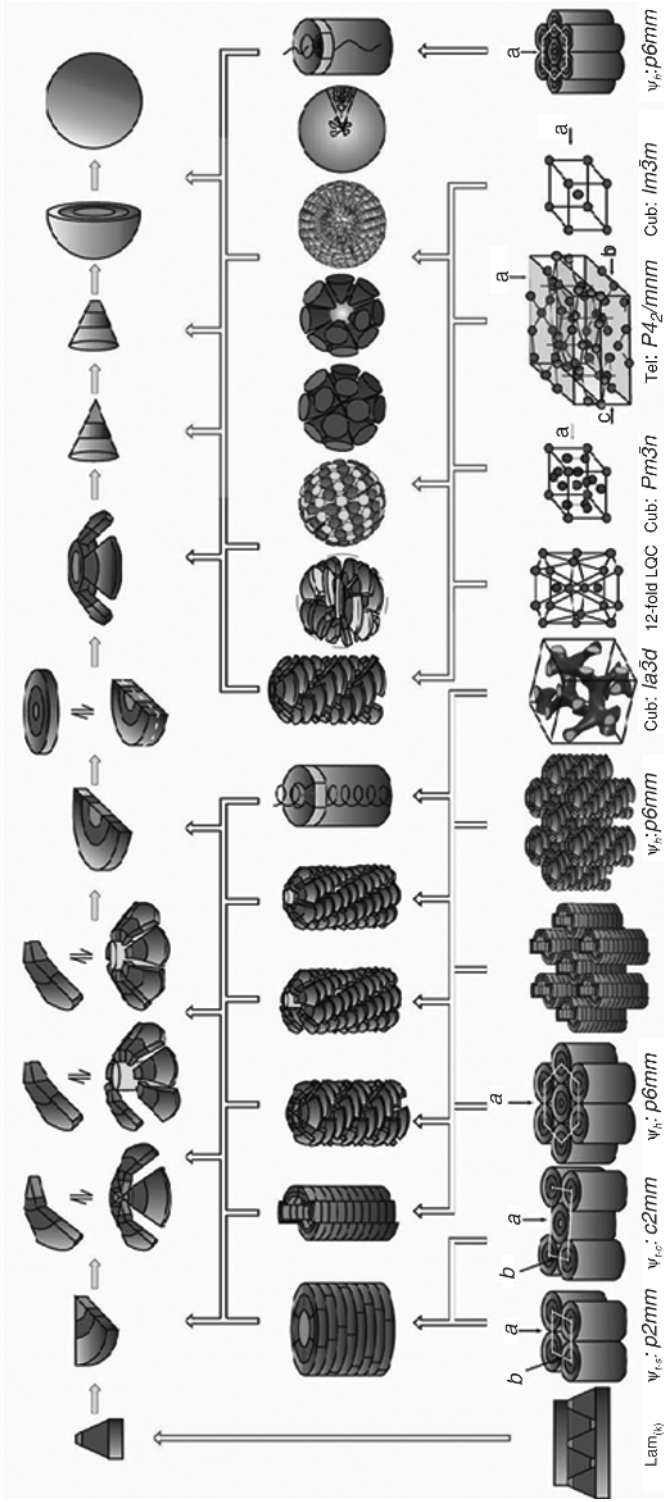
FIGURE 1.12 Periodic and quasiperiodic lattices formed via the self-assembly of Percec-type dendrons [45]. (See the color version of this figure in Color Plates section.)
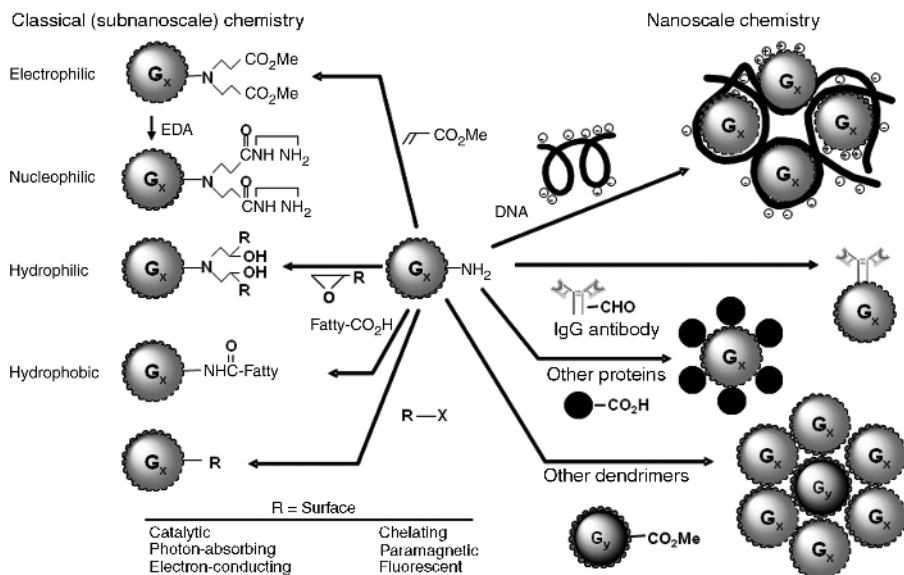
13

FIGURE 1.13   Options for modifying amine-terminated dendrimer-based nano scaffolding by utilizing classical subnanoscale and nanoscale reagents.

even at low generations due to steric effects. These unique steric effects are referred to as *nanoscale sterically induced stoichiometries* (N-SIS) [33].

The use of dendrimers as nanoscale scaffolding for MRI contrast agents was first reported by Lauterbur, Wiener, Brechbiel, and Tomalia in 1994 [47] and generated tremendous interest and activity which has been reviewed extensively elsewhere [48,49]. It involved conjugating metal-specific (i.e., gadolinium) chelating groups (i.e., DTPA or DOTA) to the terminal groups of Tomalia-type PAMAM dendrimers to produce a continuum of very precisely sized nanoparticles with well-defined nano dimensions (Figure 1.14). These surface saturated, dendrimer–metal chelates were well-characterized examples of: [dendrimer (core)-ligated metal (shell) nano-compounds]. The stoichiometries of these nano-compounds were defined accordingly as: [dendrimer]:[ligated metal]$_Z$, where $Z = N_c N_b{}^G$. These core:shell nano-compounds manifested enhancements in relaxivity properties (i.e., R_1) as a function of the dendrimer generation level and the stoichiometry of dendrimer:metal. Furthermore, the features of these soft particle–hard particle (i.e., [S-1]:[H-1] nano-compounds) fit the proposed criteria for nano-compounds described elsewhere [3,4,66]. These nano-compound possess a core derived from an [S-1] type dendrimer nano-element and shells derived from well-defined nanoscale collections of ligated metals (i.e., [H-1] type metal cluster nano-elements). Finally this series of [core:shell nano-compounds] fulfilled additional criteria that were predicted for these entities [4] by exhibiting unique emerging nano-periodic property patterns [4] as evidenced by their unprecedented high relaxivity values (i.e., R_1) that increased as a function of dendrimer generation level. Empirical formulae for members of this core: shell nano-compound series may be written as follows: $[G = 1-8]@[M]N_c N_b{}^G$.

G	1	2	3	4	5	6	7	8
Dia. (nm)	1.9	2.6	3.6	4.4	5.7	7.2	8.8	9.8
Surface groups (Z)	8	16	32	64	128	256	512	1024

Magnevist® (Commercial) ●

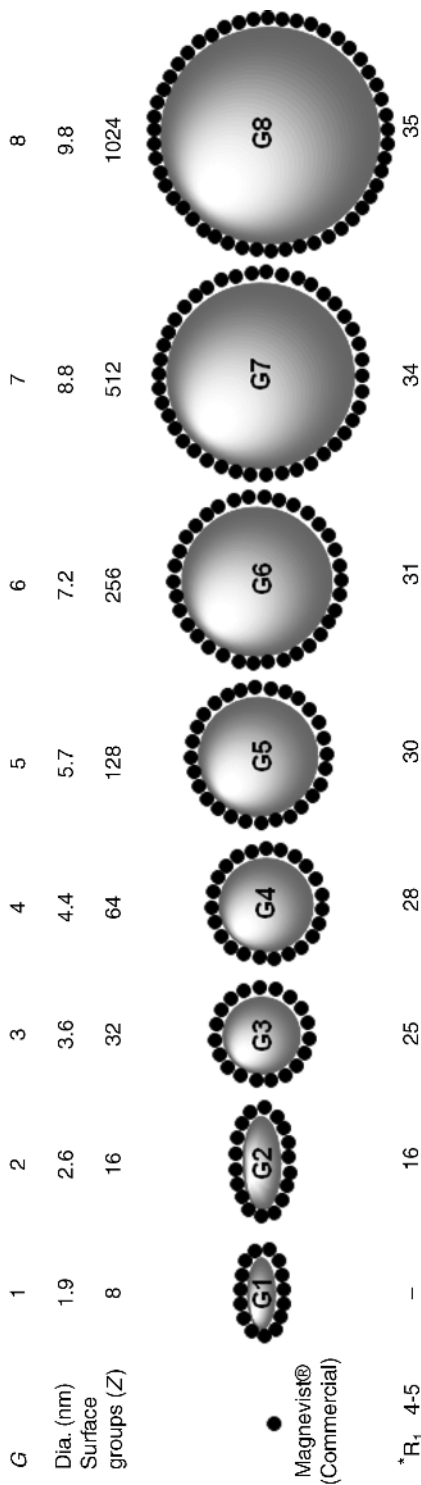| $^*R_1$ | 4-5 | — | 16 | 25 | 28 | 30 | 31 | 34 | 35 |

FIGURE 1.14 A Tomalia-type PAMAM dendrimer series (i.e., [core:1,2-diaminoethane]; (G = 1–8); {dendri-poly(amidoamine)-(metal ligation sites)$_Z$} dendrimers) illustrating; the core:shell topology, naked dendrimer scaffolding diameters (nm), number of terminal groups (Z), and relaxivity values (R_1) as a function of generation.

1.3.4   Quantized Interior Chemistry

Metal complexations with dendrimers containing nitrogen-type ligation sites have been known since the phenomenon was first observed in the earliest reported examples of the *dendri*-poly(amidoamine) (PAMAM) series [50]. More recently considerable attention has been focused on the use of certain rigid (i.e., less flexible) Yamamoto-type (i.e., *dendri*-poly(phenylazomethine) (DPA) dendrimers as nano-scale templates for assembling very well-defined metal-based nano-cluster [9] and metal oxide nanoparticles [8]. In contrast to the more flexible/less rigid nitrogen-containing PAMAM or PPI type dendrimers, the Yamamoto-type dendrimers [51] have been shown to complex and assemble a variety of metal salts in a very precise, shell by shell, sequential manner as shown in Figure 1.15. Empirical formulae describing members of this core:shell nano-compound series may be written as follows: $[M] N_c N_b^{G-1} @ [G = 4]$; where $N_c N_b^{G-1} = 4$, 12, 28, and 60, respectively. The generational shells 1–4 are saturated from the core outwardly in a sequential fashion to produce stoichiometric, dendrimer-ligated metal nano-assemblies. These nano-assemblies exhibited well-defined, mass combining ratios (i.e., dendrimer-ligated metal salt masses) reminiscent of traditional small molecule compounds. It is notable that these nano-assemblies consisted of discrete nano-module components (i.e., dendrimers and ligated metal atom collections), each of which were of nanoscale dimensions. Later it will be shown that these ligated metal domains may be transformed into precise metal nano-clusters or metal oxide nanocrystals, respectively, that remain associated as guests within their dendrimer hosts in stoichiometric proportions to produce unique core:shell nano-compounds.

1.4   HEURISTIC ATOM MIMICRY OF DENDRIMERS: *NANO-LEVEL CORE–SHELL ANALOGS OF ATOMS*

A heuristic comparison of the core–shell architectures that are present in dendrimer-based nanoscale modules and picoscale atoms was made as early as 1990 [5,6,11]. This comparison was used to point out the unique similarities that exist between aufbau components in atoms (i.e., nucleons and electrons) and those that are involved in dendrimer constructions (i.e., cores and branch-cell monomers). Remarkable analogies were also noted between dimensionally different parameters, but recognized components shared by both systems, such as (a) electron shells versus monomer shells (generations), (b) electron shell versus monomer shell aufbau filling patterns (i.e., mathematically defined), (c) electron shell versus monomer shell saturation levels, (d) atomic weights versus dendrimer molecular weights as a function of shell level and saturation level, and (e) atomic (elemental) reactivity versus dendrimer reactivity as a function of shell saturation level. We have referred to these remarkable similarities between picoscale (atomic elements) and nanoscale dendrimers as *atom mimicry*, keeping in mind that picoscale structures are best described by non-Newtonian physics, whereas, the dendrimer structures are expected to adhere to and be described by Newtonian physics. Furthermore, it appears that a very interesting
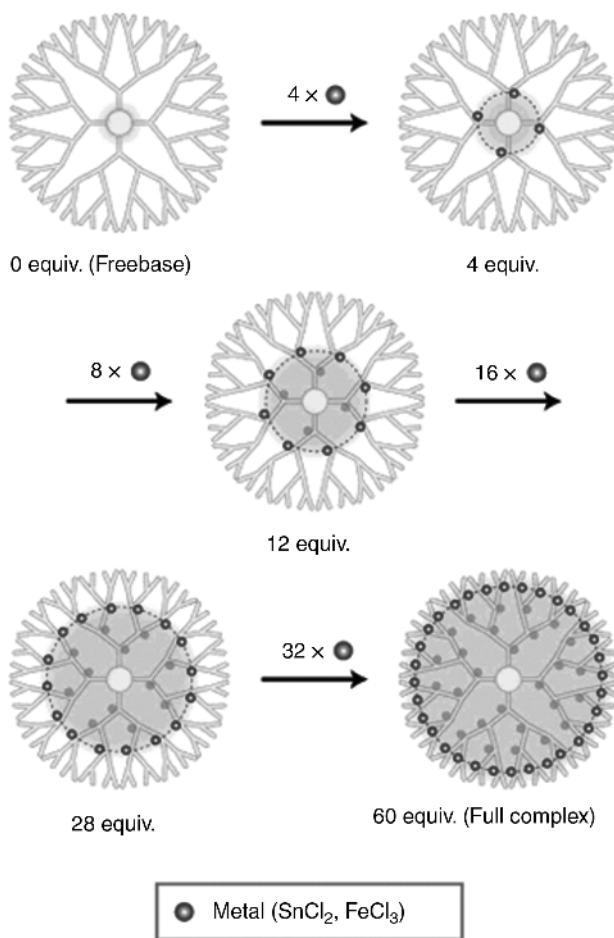
FIGURE 1.15   Schematic representation of the stepwise complexation of $SnCl_2$ or $FeCl_3$ with a Yamamoto-type dendrimer [51].

size continuum exists in the transition from picoscale (atomic) structures to nanoscale dendrimer structures as illustrated in Figure 1.16.

1.5   CHEMICAL BOND FORMATION/VALENCY AND STOICHIOMETRIC BINDING RATIOS WITH DENDRIMERS TO FORM NANO-COMPOUNDS/-ASSEMBLIES

Some of the most compelling experimental examples of dendrimer-based atom mimicry were documented with AFM. These studies clearly demonstrated the remarkably rich array of nano-assembly patterns and related stoichiometric binding
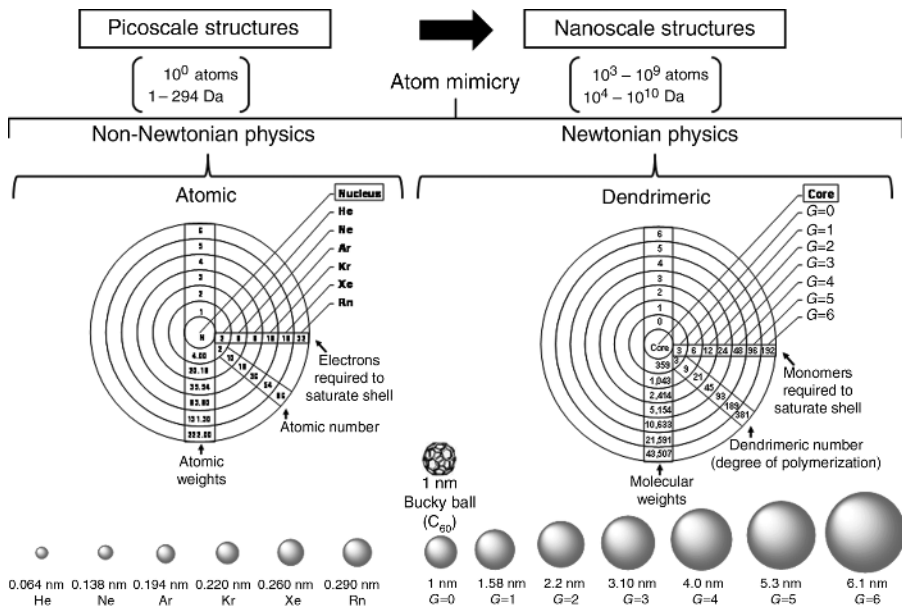
FIGURE 1.16   An example of atom mimicry. A comparison of core–shell structures representing picoscale atoms and nanoscale dendrimers, as well as the continuum of sizes that prevails over the 2-D ranges that are controlled by quantum mechanics and Newtonian physics, respectively.

ratios that were possible by simply spreading dilute solutions of amine terminated, $G = 9$; poly(amidoamine) (PAMAM) dendrimers on a mica surface with a 30° stream of argon. As shown in Figure 1.17, one can readily observe single isolated $G = 9$ modules, dimers, trimers, and a wide variety of oligomeric assemblies (i.e., mega-mers) that clearly exhibit well-defined 2-D combining ratios on the mica surface.
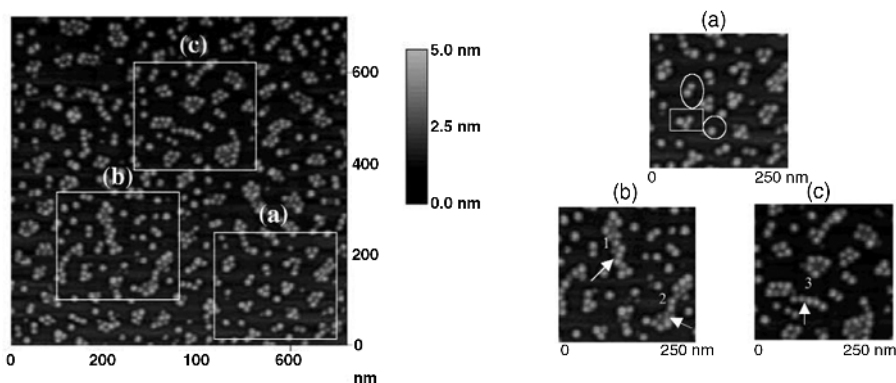

FIGURE 1.17   Tapping mode AFM images of $G = 9$: PAMAM dendrimer molecules on a mica surface [52].

Using first principles and step logic invoked by Dalton (i.e., *Philosophy for a Chemical System*, 1808) [2], as stated earlier (Figure 1.1), it was possible to experimentally demonstrate that certain quantized nano-modules (i.e., dendrimers, fullerenes, metal nano-clusters, or metal oxide nanocrystals) could be chemically combined or assembled to produce stoichiometric nano-compounds/-assemblies possessing well-defined mass combining ratios. Furthermore, both the quantized nano-modules (i.e., nano-elements) and their resulting nano-compounds were found to exhibit new emerging properties and interesting new nano-periodic property patterns [4].

Both soft matter and hard matter categories of these quantized nano-modules (i.e., referred to as nano-elements), have been proposed based on selection criteria described elsewhere [4] (Figure 1.18). Furthermore, these 12 soft and hard nano-elements, designated [S-*n*] and [H-*n*], respectively, have been reported to form a wide range of soft particle and soft–hard particle type nano-compounds. Both the nano-elements and their nano-compounds are widely recognized to exhibit new emerging properties and nano-periodic property patterns [4]. Leading references to these literature examples, designated by X in the combinatorial nano-compound library (Figure 1.18), are described in greater detail elsewhere [4]. This account will focus only on four selected examples of nano-compound formation designated by (*) that involve either reactions or self-assembly with dendrimers (Figure 1.18). Combining dendrimers (i.e., [S-1] type) nano-element categories with other dendrimers (i.e., [S-1]:[S-1]$_n$ core–shell

Soft particle nano-element categories

Dendrimers dendrons	Nano-latexes	Polymeric micelles	Proteins	Viral capsids	RNA/DNA
S-1	S-2	S-3	S-4	S-5	S-6

Hard particle nano-element categories

Metal (M^n) (nanoclusters)	Metal chalcogenide (nanocrystals)	Metal oxide nanocrystals	Silica (nanoparticles)	Fullerenes	Carbon nanotubes
H-1	H-2	H-3	H-4	H-5	H-6

Soft particle nano-compounds

Nano-elements	Dendrimers dendrons	Nano-latexes	Polymeric micelles	Proteins	Viral capsids	DNA/RNA
Dendrimers dendrons	S-1:S-1 *	S-2:S-1 X	S-3:S-1 X	S-4:S-1 X	S-5:S-1 X	S-6:S-1 X
Nano-latexes		S-2:S-2	S-3:S-2	S-4:S-2	S-5:S-2	S-6:S-2 X
Polymeric micelles		S-2:S-3	S-3:S-3	S-4:S-3	S-5:S-3	S-6:S-3 X
Proteins		S-2:S-4	S-3:S-4 X	S-4:S-4 X	S-5:S-4	S-6:S-4
Viral capsids		S-2:S-5	S-3:S-5	S-4:S-5	S-5:S-5	S-6:S-5 X
DNA/RNA		S-2:S-6	S-3:S-6	S-4:S-6	S-5:S-6 X	S-6:S-6

Soft/hard particle nano-compounds

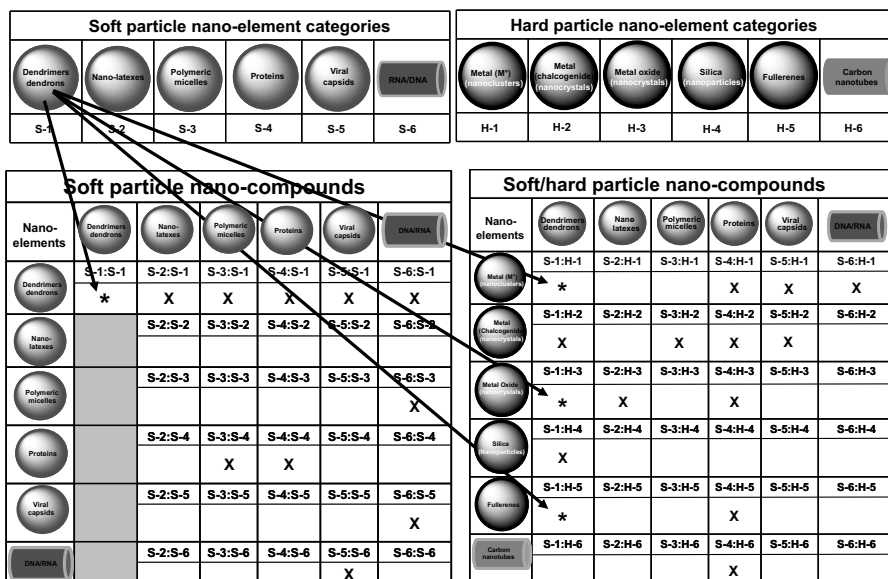| Nano-elements	Dendrimers dendrons	Nano latexes	Polymeric micelles	Proteins	Viral capsids	DNA/RNA
Metal (M^n) (nanoclusters)	S-1:H-1 *	S-2:H-1	S-3:H-1	S-4:H-1 X	S-5:H-1 X	S-6:H-1 X
Metal (Chalcogenide) (nanocrystals)	S-1:H-2 X	S-2:H-2	S-3:H-2 X	S-4:H-2 X	S-5:H-2 X	S-6:H-2
Metal Oxide (nanocrystals)	S-1:H-3 *	S-2:H-3 X	S-3:H-3	S-4:H-3 X	S-5:H-3	S-6:H-3
Silica (nanoparticles)	S-1:H-4 X	S-2:H-4	S-3:H-4	S-4:H-4	S-5:H-4	S-6:H-4
Fullerenes	S-1:H-5 *	S-2:H-5	S-3:H-5	S-4:H-5 X	S-5:H-5	S-6:H-5
Carbon nanotubes	S-1:H-6	S-2:H-6	S-3:H-6	S-4:H-6 X	S-5:H-6	S-6:H-6

FIGURE 1.18 Proposed hard and soft particle nano-element categories and combinatorial libraries of possible nano-compounds. Nano-compounds designated by [*] are described in the following section. Nano-compounds designated by [X] have been reported in the literature and described elsewhere [4].

types), with fullerenes (i.e., [S-1]:[H-5]$_n$ core–shell type), or with metal nano-clusters (i.e., [H-1]$_n$:[S-1] core–shell type) produced three unique core–shell nano-compound category types designated in Figure 1.18. On the other hand, dendrimers have also been used as templates to produce precisely sized [H-3] type, metal oxide nanocrystals which have exhibited interesting quantum size effects as described in the next section.

1.5.1 Dendrimer–Dendrimer; [S-1]:[S-1]$_n$ Core–Shell Type Nano-Compounds

Saturated shell, nano-compounds (Figure 1.19) are prepared by a two-step approach that involved: first, self-assembly of an excess of carboxylic acid terminated dendrimers (i.e., shell reagent) around a limited amount of amine-terminated dendrimer (i.e., core reagent) in the presence of LiCl. This was followed by covalent amide bond formation between the core and dendrimer shell reagents using a carbodiimide reagent [52–54]. The resulting nano-compounds (i.e., saturated core–shell tecto (dendrimers), referred to as *megamers*), are prime examples of precise poly-dendrimer cluster structures. These structures and their stoichiometries may be mathematically predicted by the Mansfield–Tomalia–Rakesh equation (Figure 1.25) [6,55] and have been unequivocally verified by experimental mass spectrometry, gel electrophoresis, and atomic force field microscopy [6,52,53,56].

1.5.2 Dendrimer–Fullerene; [S-1]:[H-5]$_n$ Core–Shell Type Nano-Compounds

Stoichiometric dendrimer core–fullerene shell nano-compounds were readily formed by allowing a [*core*: 1,2-diaminoethane]; $(G = 4)$; {*dendri*-poly(amidoamine)-$(NH_2)_{64}$} (PAMAM) dendrimer to react with an excess of buckminsterfullerene (C_{60}) [7]. In the presence of an excess of (C_{60}), only 30 (C_{60}) moieties bonded to the dendrimer surface to produce a well defined, stoichiometric [dendrimer core]: [fullerene shell nano-compound] (i.e., [S-1]:[H-5]$_n$ core–shell type) as shown in Figure 1.20. These structures were extensively characterized by MALDI-TOF, TGA,
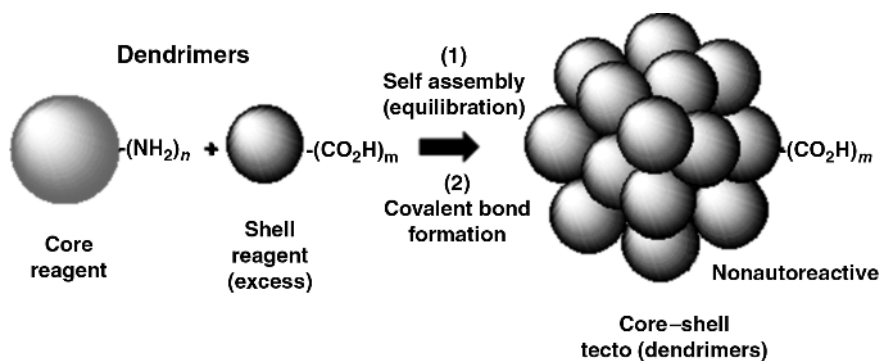

FIGURE 1.19 The saturated-shell-architecture approach to megamer synthesis. All surface dendrimers are carboxylic acid terminated [54].
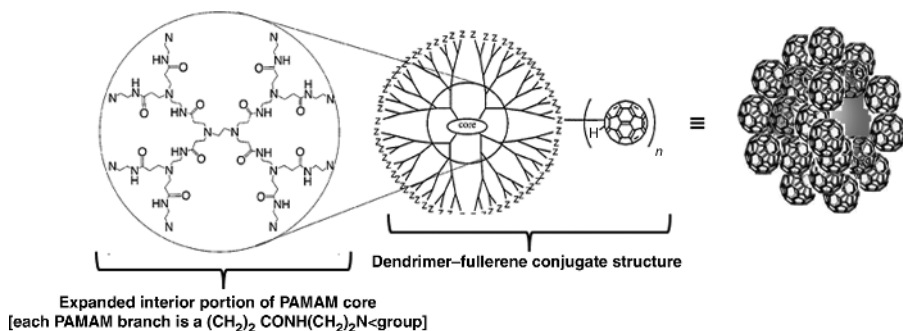
Dendrimer–fullerene conjugate structure

Expanded interior portion of PAMAM core
[each PAMAM branch is a (CH$_2$)$_2$ CONH(CH$_2$)$_2$N<group]

FIGURE 1.20   Core–shell architecture of the PAMAM core:fullerene shell; [S-1]:[H-5] core–shell type nano-compound; where: ($Z =$ terminal –NH$_2$ or–NH–, groups on the PAMAM dendrimer core component of the core–shell nano-compound) [7].

UV-vis, and FTIR. Such nano-compounds exhibited new emerging fullerene-like solubility and photo-chemical properties by readily generating singlet ($^1O_2$) in either aqueous/organic solvents. However, they offered other unique features such as larger size and nano-container type properties that would normally be associated with the dendrimer core interior.

1.5.3   Metal Nano-Cluster–Dendrimer; [H-1]$_n$:[S-1] Core–Shell Type Nano-Compounds

Using a $G = 4$, phenylazomethine dendrimer as a template, Yamamoto et al. [9] demonstrated that Pt(IV) chloride salts could be sequentially assembled to produce four discretely different, yet precise, collections of ligated Pt salts within the interior of the dendrimer. Subsequent reduction of these ligated Pt(IV) arrays yielded Pt(0) Nan clusters consisting of very *well defined numbers of Pt atoms*. The size of these incarcerated Pt(0) nano-clusters (i.e., by TEM) was in good agreement with the number of Pt atoms present in the ligated metal precursors. For example, the [H-1]$_n$:[S-1] nano-compound series designated by [Pt$_{12}$]@[G4;dendrimer], [Pt$_{28}$]@[G4;dendrimer], and [Pt$_{60}$]@[G4;dendrimer] core–shell type nomenclature were extensively characterized and determined to exhibit precise stoichiometries as described in Figure 1.21 (Where: n = 12, 28 and 60 respectively). The ability to precisely control these independently sized Pt(0) nano-cluster cores within the G4; dendrimer shells provided discrete nano-cages that prevented metal nano-cluster aggregation. Furthermore, it allowed the evaluation of these four discrete core–shell nano-compounds as catalysts in reactions involving four (4X) electron reductions of oxygen molecules. These catalytic reductions are of high interest in the development of optimized fuel cells. Quite remarkably it was demonstrated that these catalytic reductions are highly dependent on subtle metal nano-cluster size differences.

As such, a significant nano-periodic property pattern was observed within this nano-compound series. It was found that within this Pt(0) nano-cluster size continuum (i.e., sizes ranging from 0.5 to 6.0 nm) it was observed that 3 nm Pt(0) nano-cluster sizes offered optimum catalytic properties [9].
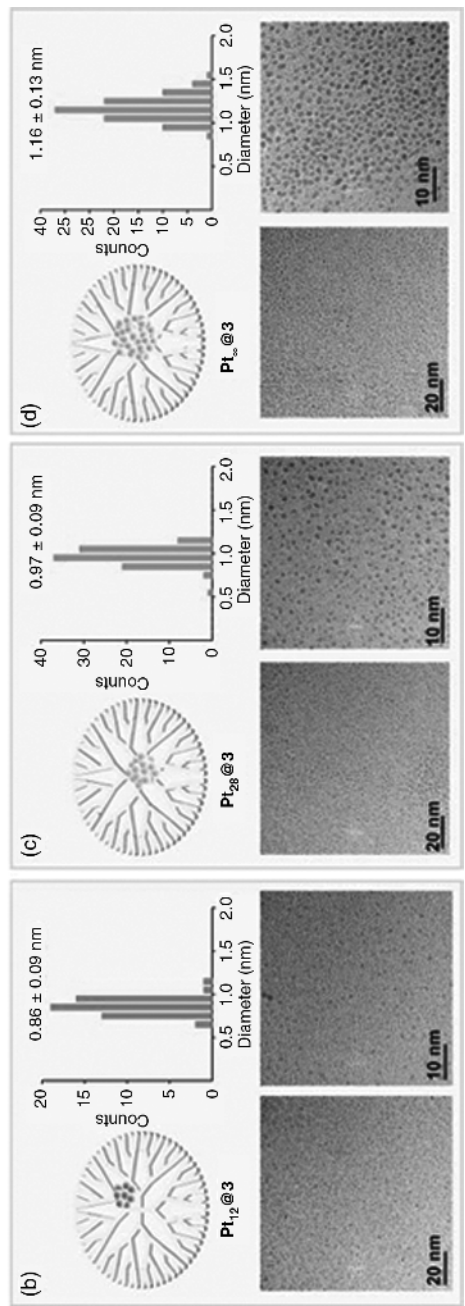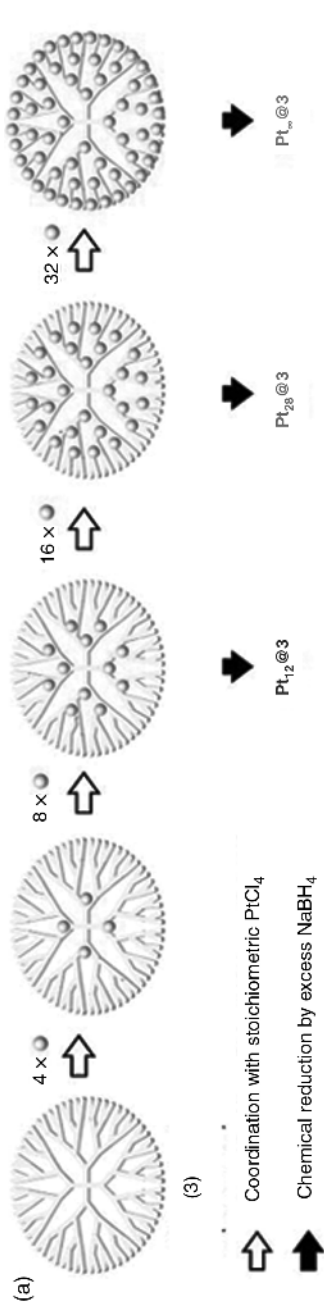
FIGURE 1.21 (a) Sequential complexation of PtCl$_4$ with a Yamamoto-type dendrimer, (3), to produce Pt$_{12}$@3, Pt$_{28}$@3, and Pt$_{60}$@3; [H-3]$_n$:[S-1] core–shell type nano-compounds, respectively, after reduction with NaBH$_4$. (b–d) Histograms of Pt(0) nano-cluster core size distributions in each nano-compound above with corresponding electromicrograms of these [H-3]$_n$:[S-1] core–shell type nano-compounds [9]. Reprinted by permission from Macmillan Publishers Ltd., *Nature Chemistry* 2009. (See the color version of this figure in Color Plates section.)
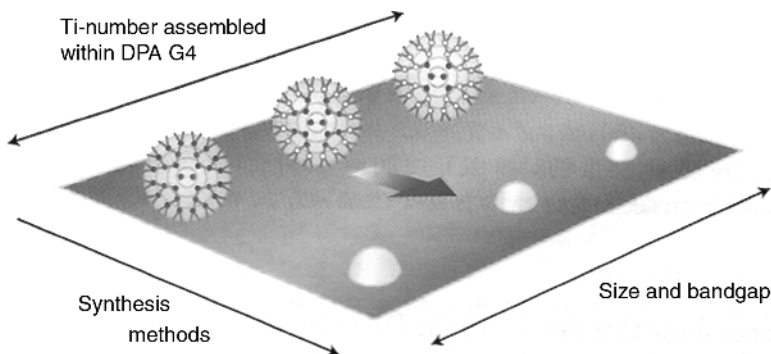
FIGURE 1.22 Illustration of the quantum size effect (Q-size) on semiconductor bandgaps for a series of well-defined $[TiO_2]_n$ nanocrystals. The nanoparticle size can be precisely controlled in a dendrimer template and is influenced by the number of $[TiO_2]_n$ assembled in a dendrimer interior. This is an elegant synthesis strategy for producing well-defined [H-3] type, metal oxide, nano-element particles [8]. Reprinted by permission from Macmillan Publishers Ltd., *Nature Nanotechnology* 2008.

1.5.4 Templated Metal Salt Nanocrystal–Dendrimer; $[H-3]_n$:[S-1] Core–Shell Nano-Compounds as Precursors to Well-Defined Metal Oxide Nanocrystals (i.e., $[TiO_2]n$, where $n = 6$, 14, and 30)

Much as described above, Yamamoto et al. [9], also demonstrated use of the rigid phenylazomethine dendrimers as templates for ligating discrete titanium salt domains within the dendrimer interior. Based on these precise assemblies, they served as precursors for producing very well-defined [H-3] type metal oxide nanocrystals (i.e., $[TiO_2]_n$, where $n = 6$, 14, and 30). The precursor $[Ti(acac)Cl_3]_n@[G4;dendrimer]$ metal ligation complexes were either hydrolyzed or thermolyzed to produce the desired *anatase* or *rutile* forms of TiO_2, with concurrent destruction of the dendrimer template. A unique quantum size effect is observed as one decreases the TiO_2 nanoscale sizes within this series. Such controlled size reductions may be used to raise the conduction band while lowering the valence bands of the metal oxide nanocrystals as illustrated in Figure 1.22. These quantum size (Q-size) effects produce a unique "*nano-periodic property pattern*," which is evidenced by a blue shift as the nanoparticle size decreases.

1.6 NANO-PERIODIC CHEMICAL/PHYSICAL PROPERTY PATTERNS

1.6.1 Periodic Chemical Reactivity/Physical Size Property Patterns

Soft particle, dendrimer-based, [S-1] type nano-elements are unique macromolecules that exhibit completely different physicochemical properties (i.e., nano-periodic property patterns) compared to traditional polymers. This is largely due to congestion properties that emerge as a function of generational growth, as shown in Figure 1.23,
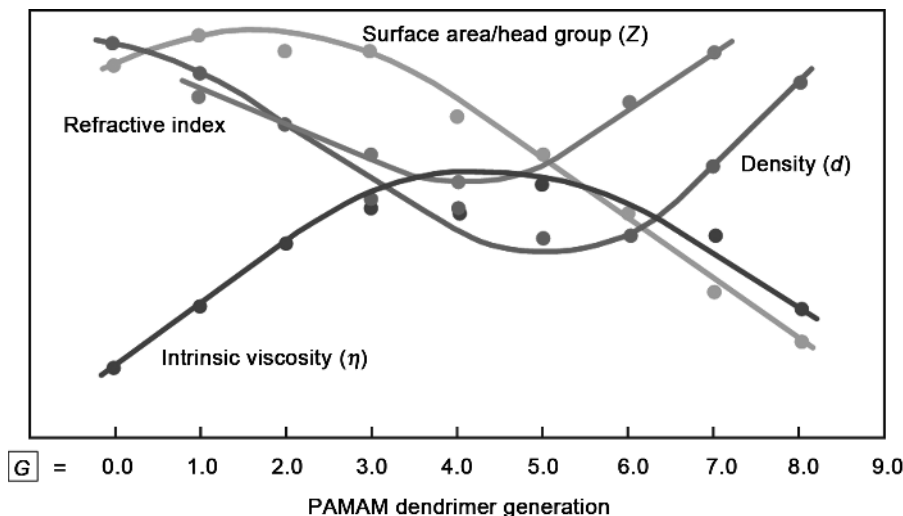
FIGURE 1.23   Comparison of surface area/head group (Z), refractive index, density (d), and viscosity (η) as a function of generation: G = 1–9 [11]. Copyright Wiley-VCH Verlag GmbH & Co. KGaA.

to produce unprecedented nano-periodic property patterns that are intrinsic and uniquely characteristic of dendrimers.

Plots of intrinsic viscosity [η], density (d), surface area per Z group (A_Z), and refractive index, as a function of generation, clearly show intrinsic maxima or minima at generations = 3–5 for this Tomalia-type PAMAM dendrimer series. These data corroborate computer-assisted molecular-simulation predictions [11,57], and extensive photochemical probe experiments reported by Turro et al. [18,58–62].

Dendrimer-based intrinsic viscosities [η] initially increase in a classical fashion as a function of molar mass (generation), but dramatically decline beyond a critical generation due to a congestion-induced shape change. A dendrimer shape change occurs from an extended, compressible, floppy configuration in the early generations (i.e., G = 0–3) to more rigid globular shapes in the later generations (i.e., G = 4–10). In effect, at critical generations (i.e., G = 3–4 and >) the dendrimer acts more like an Einstein spheroid. Intrinsic viscosity is a physical property expressed in dL/g, which in essence is the ratio of volume to mass. As the generation number increases and transition occurs to a spherical shape, the volume of the spherical dendrimer increases in cubic fashion while its mass increases exponentially; hence, the value of [η] must decrease once a certain generation is reached. This prediction has now been widely confirmed for many different dendrimer families [11,25,63]. Dendrimer surface congestion may be appraised mathematically as a function of generation according to the following simple relationship:

$$A_Z = \frac{A_D}{N_Z} \alpha \frac{r^2}{N_c N_b^G}$$

where A_Z is the surface area per terminal group Z, A_D the dendrimer surface area, and N_Z the number of surface groups Z per generation. This relationship predicts the surface area per Z group at higher generations (G) and becomes increasingly smaller as it finally approaches the cross-sectional area or van der Waals dimension of the surface groups Z at higher generations. Congestion at these higher generations (G) is referred to as "*de Gennes dense-packing*" [11]. Ideal dendritic growth without branch defects is possible only for those generations preceding this dense-packed state. This critical dendrimer property gives rise to self-limiting dendrimer dimensions, which are a function of the branch-cell segment length (I), the core multiplicity N_c, the branch-cell juncture multiplicity N_b, and the steric dimensions of the terminal group Z. Dendrimer radius r in the above expression is dependent on the branch-cell segment lengths l; wherein, large l values delay congestion. On the other hand, larger N_c, N_b values and larger Z dimensions dramatically enhance congestion. These congestion properties are unique for each dendrimer family; wherein N_c and N_b determine the generation levels within a family that will exhibit nano-encapsulation properties. Higher N_c and N_b values predict that lower generation levels will produce appropriate surface congestion properties to manifest encapsulation features as shown in Figure 1.24.

1.6.2 Spheroidal Valency Defined by Nano-Sterics

Clearly these fundamental dendrimer properties illustrate the unique and intrinsic nano-periodic property patterns manifested by this soft matter, [S-1] type nano-element category. Many other nano-periodic property patterns have been documented for the behavior, assembly, and reactions of dendrimers with other dendrimers and with other well-defined nano-element categories. For example, work on this soft matter, [S-1] type nano-element category [6,52,55] has demonstrated that mathematically defined, periodic size properties of spheroidal dendrimers can determine chemical reactivity patterns with other dendrimers. These reactivity patterns, based on the relative sizes of a targeted dendrimer cores and dendrimer shell components, strongly influence the assembly of precise dendrimer clusters (i.e., core–shell (tecto) dendrimers). Mathematical relationships (i.e., the *Mansfield–Tomalia–Rakesh equation*) predict dendrimer cluster saturation levels (i.e., magic numbers for dendrimer shells) as a function of the core dendrimer size relative to the size of the shell dendrimers that are being used to construct the dendrimer cluster (Figure 1.25) [55,64]. These periodic property patterns and magic shell relationships are reminiscent of those observed for the self assembly of [H-1] type metal nanocrystals; wherein, the predicted number of touching spheroids surrounding a central core metal atom is 12 as shown below (Figure 1.25), when $r_1/r_2 = 1.00$.

1.6.3 Atom Mimicry and Nano-Periodic Property Patterns Observed for Yamamoto-Type Dendrimers

The importance of controlling the CNDP's related to flexibility/rigidity was clearly demonstrated with Yamamoto-type dendrimers. Based on the rigidity features and
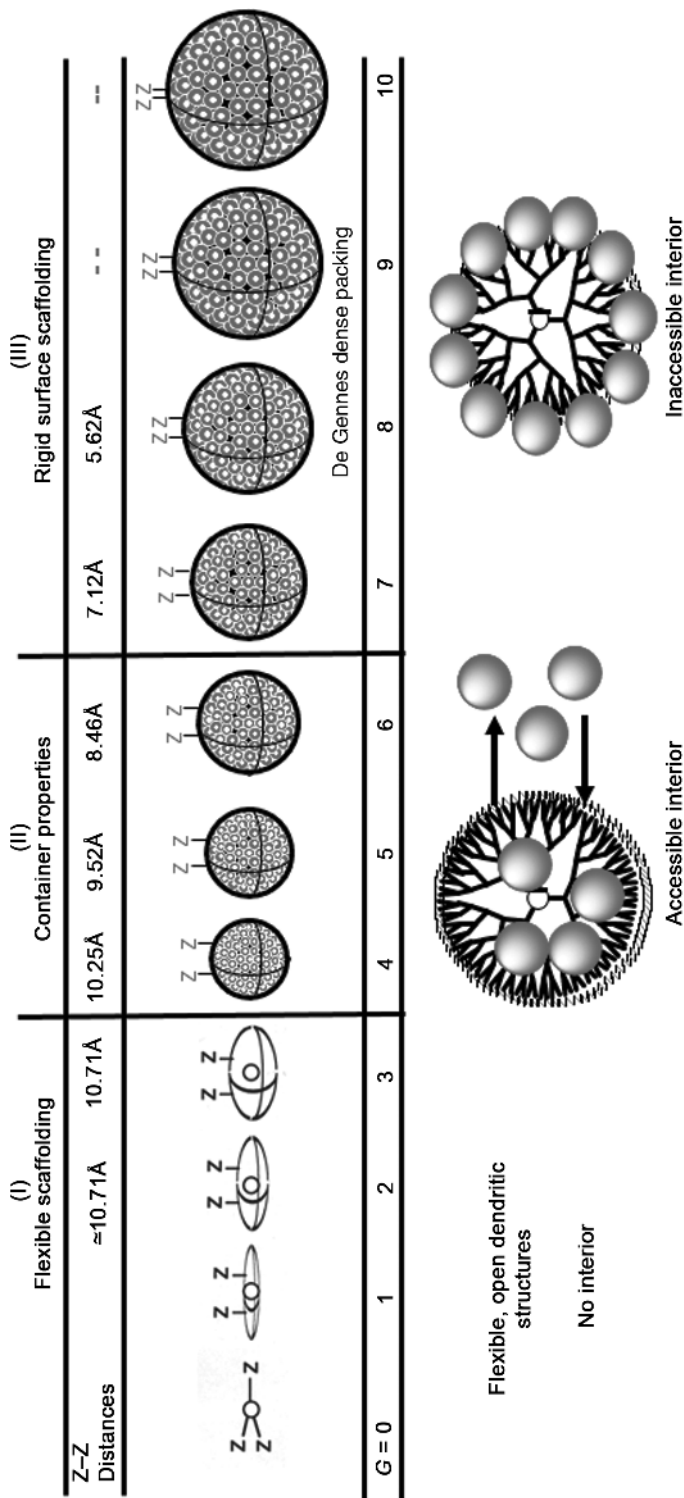
	(I) Flexible scaffolding			(II) Container properties			(III) Rigid surface scaffolding			
Z–Z Distances	≈10.71Å		10.71Å	10.25Å	9.52Å	8.46Å	7.12Å	5.62Å	- -	- -
G = 0	1	2	3	4	5	6	7	8	9	10

De Gennes dense packing

Flexible, open dendritic structures

No interior

Accessible interior

Inaccessible interior

FIGURE 1.24 Congestion-induced dendrimer shape changes (I, II, and III) with development of nanocontainer properties for a family of [*core*:1,2-diaminoethane]; {*dendri*-poly(amidoamine)-(NH$_2$)$_Z$}, (PAMAM) dendrimers: $N_c = 4$; $N_b = 2$, where Z–Z = distance between surface groups as a function of generation.
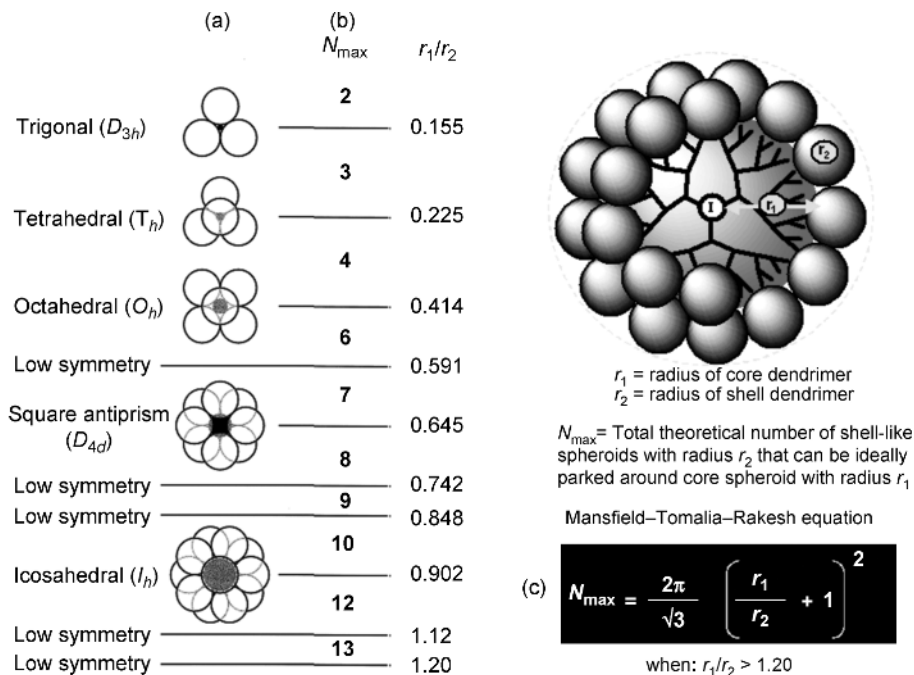
FIGURE 1.25 (a) Symmetry properties of core–shell tecto(dendrimer) structures, when: $r_1/r_2 < 1.20$. (b) Sterically induced stoichiometry (SIS) defined shell capacities (N_{max}), based on the respective core and shell radii, when: $r_1/r_2 < 1.20$. (c) Mansfield–Tomalia–Rakesh equation for calculating the maximum shell filling value (capacity) (N_{max}), when: $r_1/r_2 > 1.20$ [6,55].

mathematically quantized ligation sites present in Yamamoto-type dendrimers, it was possible to quantitatively document an amazing sequence of metal–dendrimer shell filling events. These metal-shell filling events are heuristically reminiscent of traditional electron-shell filling events observed for elemental atoms. It was shown in this present case that quantized amounts of metal salts will first ligate closest to the core at the lowest generation level to produce a saturated generational shell with well-defined and perfect stoichiometry (i.e., $4 \times @G = 1$), based on ligation sites present. Subsequent addition of metal reagent led to a stepwise filling of the next highest generational shell until it reached a shell-saturated state (i.e., $8 \times @G = 2$) and higher generation saturation states as shown in Figure 1.26.

1.7 FIRST STEPS TOWARD A "CENTRAL DOGMA" FOR SYNTHETIC NANO-CHEMISTRY? DENDRIMER-BASED NANO-CHEMISTRY

As stated earlier (Figure 1.1), the "central dogma" for traditional soft matter chemistry emerged from the first initiatives of Lavoisier and Dalton in the early nineteenth
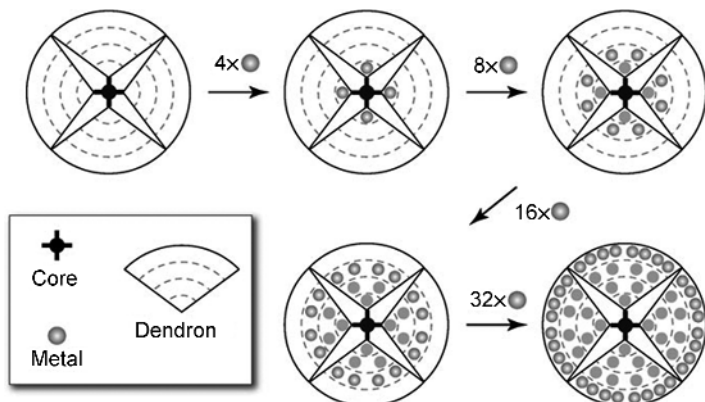
FIGURE 1.26   A Yamamoto-type poly(phenylazomethine) dendrimer series illustrating quantized, sequential dendrimer shell filling with metal salts using; [$G = 4$]; {*dendri*-poly(phenylazomethine)} (DPA) dendrimers [65]. Copyright Wiley-VCH Verlag Gmbh & Co. KGaA.

century and was initially focused on the simple combinatorial bonding of atoms to form small molecules (i.e., monomers, branch-cell monomers), much as illustrated in Figure 1.28. Synthetic soft matter chemistry throughout the nineteenth and twentieth century witnessed steady progress toward more complex molecular structure and architecture, including dendrons and dendrimers. Figure 1.28 illustrates the "aufbau process" for the bottom-up construction of such well-defined nanoscale structures (i.e., dendrons/dendrimers), which one might refer to as soft matter nano-elements [3,4,66]. Essentially all other proposed hard–soft nano-element categories
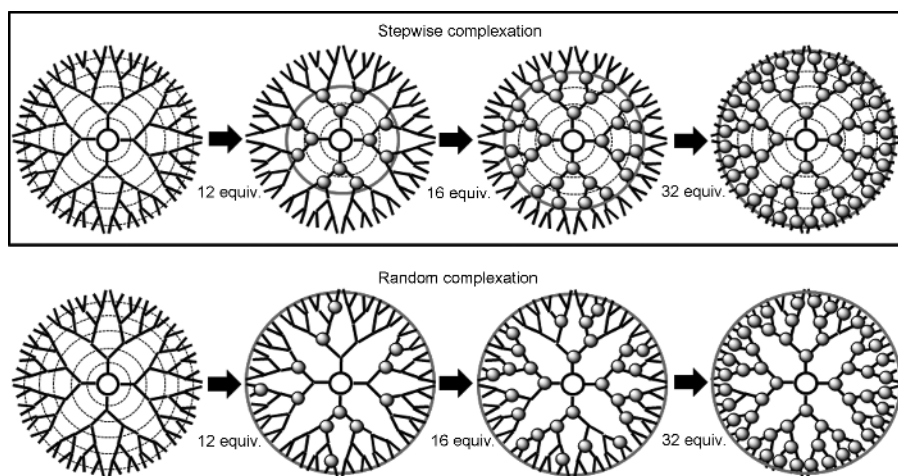
FIGURE 1.27   A comparison of stepwise and random ligation processes that are observed for PtCl$_4$ complexation with a rigid Yamamoto-type poly(phenylazomethine) dendrimer and a flexible Tomalia-type poly(amidoamine) (PAMAM) dendrimer, respectively [8].
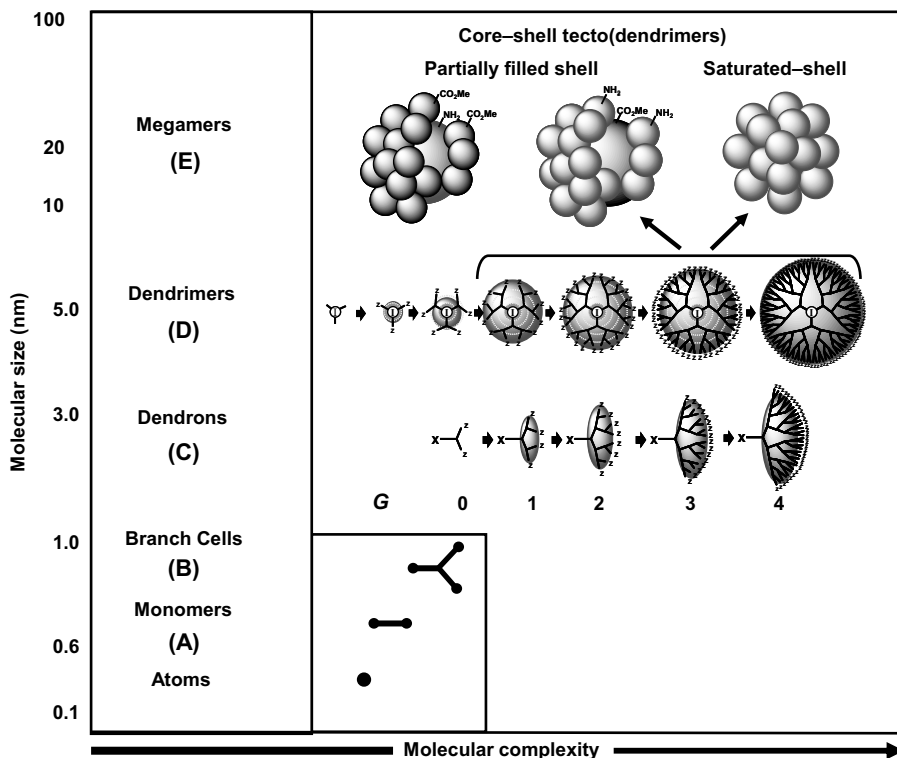
FIGURE 1.28 Approximate nanoscale dimensions as a function of hierarchical building blocks (i.e., atoms, monomers, branch cells, dendrimers, and megamers) and presumed conservation of critical hierarchical design parameters.

(Figure 1.18) evolve from an analogous aufbau strategy that allows the control and conservation of critical hierarchical design parameters from the atom to the nanoscale level (i.e., CADP → CMDP → CNDP). Vivid examples of such aufbau processes for two hard matter nano-element categories (i.e., [H-1] and [H-2] types) were described earlier (see Figures 1.21 and 1.22). In each case, metal atoms were precisely controlled and assembled to produce both [H-1] type metal nano-clusters or [H-3] type metal oxide nanocrystals by using soft matter [S-1] type nano-element (i.e., dendrimer structures) as templates. Nature has already presented very exquisite evolutionary aufbau strategies for synthesizing proposed soft matter nano-element categories such as (a) proteins [S-4], (b) viral capsids [S-5], and (c) DNA/RNA [S-6] (see Figure 1.18).

Clearly a deeper understanding of the critical "aufbau processes" leading to each of these well-defined nano-element categories, and their interconnections within a larger picture (i.e., a nano-periodic system) should be expected to provide important first steps toward the evolution of a central dogma for the new emerging area of *synthetic nano-chemistry*.

1.8   CONCLUSIONS

In this account, we have presented several examples of atom mimicry that have been observed for dendrimers (i.e., quantized nano-element-like behavior). It is apparent that the conservation and control of critical hierarchical design parameters (i.e., size, shape, surface chemistry, flexibility, and architecture) from the atomic ($\sim$0.001 nm) to the nanoscale level (i.e., 1–100 nm) are intrinsic and well-defined features (see Figures 1.23–1.25) of dendrimers (Figure 1.28). These structure-controlled CNDPs are important parameters that define chemical bonding, self-assembly (Figure 1.12) [45,46], stoichiometries (Figures 1.21, 1.26, and 1.27), nano-steric effects (Figure 1.25), and architectural patterns that are observed when combining dendrimers with other well-defined nano-modules. These new emerging properties and nano-periodic property patterns associated with dendrimers and their nano-compounds are distinctly different, yet reminiscent of similar features observed for their hierarchical precursors (i.e., atomic elements and small molecules). Many of these early observations on dendrimers inspired our more comprehensive proposal to view and classify all well-defined nanoparticles (i.e., hard and soft matter) that fit similar atom mimicry criteria [3,4,66]. It is from this perspective and based on first principles and rationale invoked for traditional chemistry, that we take initial steps toward a deeper understanding of the implications and possibilities for this new emerging area of *synthetic nano-chemistry*. It goes without saying that this new field
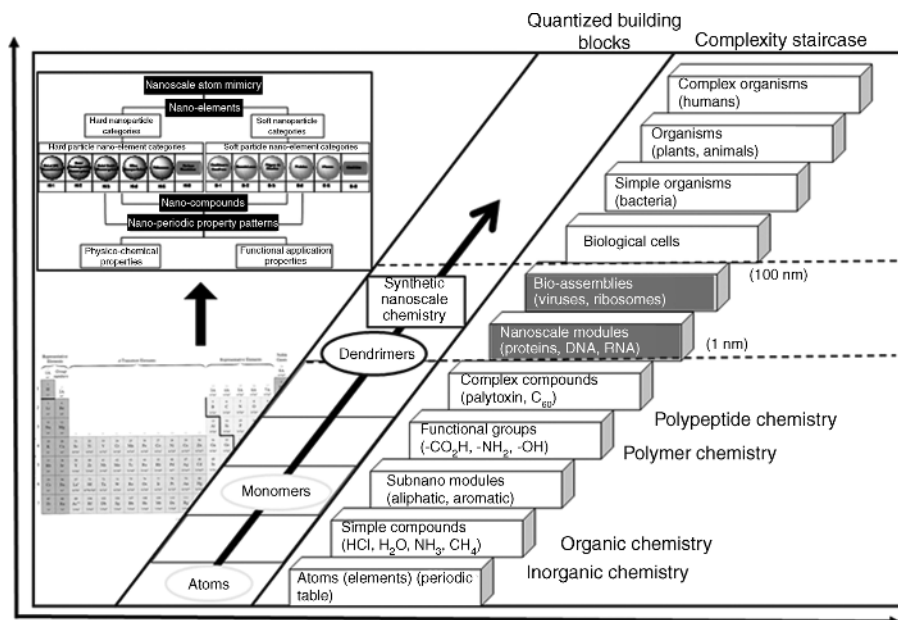

FIGURE 1.29   A chronological overview of traditional disciplines, structural complexity, and quantized building blocks relative to traditional and nano-periodic systems.

will be built on the shoulders of earlier traditional synthesis disciplines as described in Figure 1.29.

> Finally, the spirit of this perspective is not to advocate the disruption/violation of any natural physicochemical laws, but to encourage new and different thinking steeped in historical first principles which may evolve into a comprehensive systematic framework for unifying nanoscience. Much more remains to be done.
>
> Donald A. Tomalia

ACKNOWLEDGMENTS

REFERENCES

[1] R. Hoffmann, *Angew. Chem. Int. Ed.* **1987**, *26*, 846.

[2] E. Heilbronner, J. D. Dunitz, *Reflections on Symmetry*, VCH Publishers, Inc., New York, **1993**.

[3] D. A. Tomalia, *National Science Foundation Final Workshop Report* **2008**, p. 1.

[4] D. A. Tomalia, *J. Nanopart. Res.* **2009**, *11*, 1251.

[5] D. A. Tomalia, *Adv. Mater.* **1994**, *6*, 529.

[6] D. A. Tomalia, *Prog. Polym. Sci.* **2005**, *30*, 294.

[7] A. W. Jensen, B. S. Maru, X. Zhang, D. Mohanty, B. D. Fahlman, D. R. Swanson, D. A. Tomalia, *NanoLetters* **2005**, *5*, 1171.

[8] N. Satoh, T. Nakashima, K. Kamikura, K. Yamamoto, *Nat. Nanotechnol.* **2008**, *3*, 106.

[9] K. Yamamoto, T. Imaoka, W.-J. Chun, O. Enoki, H. Katoh, M. Takenaga, A. Sonoi, *Nat. Chem.* **2009**, *1*, 397.

[10] D. A. Tomalia, J. M. J. Fréchet, *J. Polym. Sci. Part A Polym. Chem.* **2002**, *40*, 2719.

[11] D. A. Tomalia, A. M. Naylor, W. A. Goddard III, *Angew. Chem. Int. Ed. Engl.* **1990**, *29*, 138.

[12] F. Zeng, S. C. Zimmerman, *Chem. Rev.* **1997**, *97*, 1681.

[13] A. Carlmark, C. Hawker, A. Hult, M. Malkoch, *Chem. Soc. Rev.* **2009**, *38*, 352.

[14] Y. Ma, S. V. Kolotuchin, S. C. Zimmerman, *J. Am. Chem. Soc.* **2002**, *124*, 13757.

[15] J.-P. Majoral, A.-M. Caminade, *Chem. Rev.* **1999**, *99*, 845.

[16] P. Antoni, Y. Hed, A. Nordberg, D. Nystrom, H. von Holst, A. Hult, M. Malkoch, *Angew. Chem. Int. Ed.* **2009**, *48*, 2126.

[17] R. Esfand, D. A. Tomalia, in *Dendrimers and Other Dendritic Polymers* (Eds.: J. M. J. Fréchet, D. A. Tomalia), Wiley, Chichester, **2001**, p. 587.

[18] J. M. J. Fréchet, D. A. Tomalia, *Dendrimers and Other Dendritic Polymers*, Wiley, Chichester, **2001**.

[19] M. H. P. Van Genderen, M. H. A. Mak, D. B.-V. D. Berg, E. W. Meijer, in *Dendrimers and Other Dendritic Polymers* (Eds.: J. M. J. Fréchet, D. A. Tomalia), Wiley, Chichester, **2001**, p. 605.

[20] D. A. Tomalia, S. A. Henderson, M. S. Diallo, S. A. Henderson, in *Handbook of Nanoscience, Engineering and Technology* (Eds.: W. A. GoddardIII, D. W. Brenner, S. E. Lyshevski, G. J. Iafrate), CRC Press, Boca Raton, FL, **2007**, p. 24.1.

[21] M. Higuchi, S. Shiki, K. Ariga, K. Yamamoto, *J. Am. Chem. Soc.* **2001**, *123*, 4414.

[22] J. C. Hummelen, J. L. J. van Dongen, E. W. Meijer, *Chem. Eur. J.* **1997**, *3*, 1489.

[23] R. Yin, Y. Zhu, D. A. Tomalia, *J. Am. Chem. Soc.* **1998**, *120*, 2678.

[24] R. Moors, F. Vogtle, *Chem. Ber.* **1993**, *126*, 2133.

[25] J. M. J. Fréchet, *Science* **1994** *263*, **1710**.

[26] G. R. Newkome, C. N. Moorfield, F. Vögtle, *Dendritic Molecules*, VCH, Weinheim, **1996**.

[27] C. J. Hawker, J. M. J. Fréchet, *J. Am. Chem. Soc.* **1990**, *112*, 7638.

[28] P. R. Dvornic, D. A. Tomalia, *Macromol. Symp.* **1995**, *98*, 403.

[29] G. J. Kallos, D. A. Tomalia, D. M. Hedstrand, S. Lewis, J. Zhou, *Rapid Commun. Mass Spectrom.* **1991**, *5*, 383.

[30] H. M. BrothersII, L. T. Piehler, D. A. Tomalia, *J. Chromatogr. A* **1998**, *814*, 233.

[31] C. A. Cason, S. A. Oehrle, T. A. Fabre, C. D. Girten, K. A. Walters, D. A. Tomalia, K. L. Haik, H. A. Bullen, *J. Nanomater.* **2008**, *2008, Article ID 456082*.

[32] A. Sharma, A. Desai, R. Ali, D. A. Tomalia, *J. Chromatogr. A* **2005**, *1081*, 238.

[33] D. R. Swanson, B. Huang, H. G. Abdelbady, D. A. Tomalia, *New J. Chem.* **2007**, *31*, 1368.

[34] P. Singh, *Bioconjugate Chem.* **1998**, *9*, 54.

[35] P. Singh, in *Dendrimers and Dendritic Polymers* (Eds.: J. M. J. Fréchet, D. A. Tomalia), Wiley, Chichester, **2001**, p. 463.

[36] D. A. Tomalia, B. Huang, D. R. Swanson, H. M. BrothersII, J. W. Klimash, *Tetrahedron* **2003**, *59*, 3799.

[37] L. A. Kubasiak, D. A. Tomalia, in *Polymeric Gene Delivery Principles and Applications* (Ed.: M. M. Amiji), CRC Press, Boca Raton, FL, **2005**, p. 133.

[38] U. Boas, J. B. Christensen, P. M. H. Heegaard, *Dendrimers in Medicine and Biotechnology*, The Royal Society of Chemistry, Cambridge, UK, **2006**.

[39] C. Zhang, D. A. Tomalia, in *Dendrimers and Other Dendritic Polymers* (Eds.: J. M. J. Fréchet, D. A. Tomalia), Wiley, Chichester, **2001**, p. 239.

[40] J. L. Jackson, H. D. Chanzy, F. P. Booy, B. J. Drake, D. A. Tomalia, B. J. Bauer, E. J. Amis, *Macromolecules* **1998**, *31*, 6259.

[41] J. Li, D. A. Tomalia, in *Dendrimers and Other Dendritic Polymers* (Eds.: J. M. J. Fréchet, D. A. Tomalia), Wiley, Chichester, **2001**, p. 285.

[42] A. Sharma, M. Rao, R. Miller, A. Desai, *Anal. Biochem.* **2005**, *344*, 70.

[43] A.-D. Schluter, P. J. Rabe, *Angew. Chem. Int. Ed.* **2000**, *39*, 865.

[44] J. G. Rudick, V. Percec, *Accts. Chem. Res.* **2008**, *41*, 1641.

[45] V. Percec, B. C. Won, M. Peterca, P. A. Heiney, *J. Am. Chem. Soc.* **2007**, *129*, 11265.

[46] V. Percec, W.-D. Cho, G. Ungar, D. J. P. Yeardley, *J. Am. Chem. Soc.* **2000**, *122*, 10273.

[47] E. C. Wiener, M. W. Brechbiel, H. M. Brothers II, R. L. Magin, O. A. Gansow, D. A. Tomalia, P. C. Lauterbur, *Magn. Reson. Med.* **1994**, *31*, 1.

[48] W. Andra, H. Nowak, *Magnetism in Medicine: A Handbook*, Wiley-VCH Verlag Gmbh & Co. KGaA, Berlin, **2006**.

[49] R. B. Lauffer, *Chem. Rev.* **1987**, *87*, 901.

[50] D. A. Tomalia, H. Baker, J. Dewald, M. Hall, G. Kallos, S. Martin, J. Roeck, J. Ryder, P. Smith, *Polym. J. (Tokyo)* **1985**, *17*, 117.

[51] T. Imaoka, R. Tanaka, S. Arimoto, M. Sakai, M. Fujii, K. Yamamoto, *J. Am. Chem. Soc.* **2005**, *127*, 13896.

[52] D. A. Tomalia, S. Uppuluri, D. R. Swanson, J. Li, *Pure Appl. Chem.* **2000**, *72*, 2343.

[53] T. A. Betley, J. A. Hessler, A. Mecke, M. M. Banaszak Holl, B. G. Orr, S. Uppuluri, D. A. Tomalia, J. R. Baker Jr., *Langmuir* **2002**, *18*, 3127.

[54] S. Uppuluri, L. T. Piehler, J. Li, D. R. Swanson, G. L. Hagnauer, D. A. Tomalia, *Adv. Mater.* **2000**, *12*(11), 796.

[55] M. L. Mansfield, L. Rakesh, D. A. Tomalia, *J. Chem. Phys.* **1996**, *105*, 3245.

[56] S. Uppuluri, D. R. Swanson, H. M. Brothers II, L. T. Piehler, J. Li, D. J. Meier, G. L. Hagnauer, D. A. Tomalia, *Polym. Mater. Sci. Eng. (ACS)* **1999**, *80*, 55.

[57] I. Tanis, D. Tragoudaras, K. Karatasos, S. H. Anastasiadis, *J. Phys. Chem. B* **2009**, *113*, 5356.

[58] O. Enoki, H. Katoh, K. Yamamoto, *Org. Lett.* **2006**, *8*, 569.

[59] K. R. Gopidas, A. R. Leheny, G. Caminati, N. J. Turro, D. A. Tomalia, *J. Am. Chem. Soc.* **1991**, *113*, 7335.

[60] J. Jockusch, J. Ramirez, K. Sanghvi, R. Nociti, N. J. Turro, D. A. Tomalia, *Macromolecules* **1999**, *32*, 4419.

[61] M. F. Ottaviani, N. J. Turro, S. Jockusch, D. A. Tomalia, *J. Phys. Chem.* **1996**, *100*, 13675.

[62] N. J. Turro, J. K. Barton, D. A. Tomalia, *Acc. Chem. Res.* **1991**, *24*(11), 332.

[63] A.-M. Caminade, R. Laurent, J.-P. Majoral, *Adv. Drug Deliv. Rev.* **2005**, *57*, 2130.

[64] D. A. Tomalia, J. M. Frechet, *Prog. Polym. Sci.* **2005**, *30*, 217.

[65] T. Imaoka, R. Tanaka, K. Yamamoto, *Chem. Eur. J.* **2006**, *12*, 7328.

[66] D. A. Tomalia, *Soft Matter,* **2010**, *6*, 456.